Letters in Applied NanoBioScience
Open-Access Journal (ISSN: 2284-6808)

Article
Volume 13, Issue 4, 2024, 178
https://doi.org/10.33263/LIANBS134.178

Novel M-Polynomials for Computing Graph Invariants of Certain Drugs: Targeting COVID-19 and Omicron

Melaiyur Sankarraman Srinivasan [1,*], Ranjan Helen [1]

[1] PG & Research Department of Mathematics, Poompuhar College (Autonomous) (Affiliated to Bharathidasan University, Tiruchirappalli), Melaiyur - 609107, Tamil Nadu, India; mssn84@gmail.com (M.S.S.); helenranjan@gmail.com (R.H);
* Correspondence: mssn84@gmail.com (M.S.S.);

Scopus Author ID 57372448200

Received: 20.08.2023; Accepted: 14.05.2024; Published: 27.08.2024

Abstract: COVID-19 is a life-threatening disease caused by the novel coronavirus (SARS-CoV-2), propagating rapidly over the world. Omicron, a new variant identified in SARS-CoV-2 lineage B.1.1.529, has a whopping 32 mutations in the spike protein alone, which turns out to be a global concern recently. Being computational approaches, graph invariants are a bridging tool among science and technology, particularly in structural chemistry, computer networks, and pharmacopeia. Topological indices (TIs) are numeric quantities that have been frequently employed as graph invariants for symmetries, distances connecting vertices, and degrees of vertices. Mathematical investigations of such TIs may assist in determining their applicability to pharmacological properties. Obtaining the TIs of a network via M-polynomial would be a promising approach. Herein, we define Lakvir indices, a novel class of node degree-based TIs, and explore their derivations via Lakvir M-Polynomials (LM Polynomials) for certain drugs employed in the treatment of COVID-19 and Omicron.

Keywords: COVID-19; Omicron; Remdesivir; Molnupiravir; Lakvir index; Lakvir degree.

1. Introduction

Numerous viral diseases have begun to evolve, posing a severe public health threat. In 2002 and 2003, severe acute respiratory coronavirus syndrome (SAR-CoV) was observed, and H1N1 influenza was reported in 2009 [1-4]. The present coronavirus disease 2019 (COVID-19), identified as a global pandemic, has challenged the public healthcare systems of most afflicted countries [5-8]. Coronaviruses are single-stranded RNA viruses that are positive-sense and enveloped [9]. The novel coronavirus known as severe acute respiratory syndrome coronavirus 2 (SARS-CoV-2) causes COVID-19. SARS-CoV-2, a beta coronavirus with proteins. Complications of SARS-CoV-2 infection can range from moderate to severe, including cough, fever, rhinorrhea, sore throat, septic shock, and severe pneumonia [10-13] (Figure 1). The WHO declared COVID-19 disease as a pandemic on March 11, 2020, after it expanded swiftly around the world. Up till now, there is no specific antiviral medicine capable of absolutely curing COVID-19 disease. However, existing antiviral drugs such as Arbidol, Remdesivir, Theaflavin, Favipiravir, and Darunavir suppress protease inhibitors as well as nucleoside or nucleotide analogs that hinder viral RNA synthesis were repurposed to combat the COVID-19 pandemic [14,15].

Arbidol, identified as an antiviral medication of non-nucleoside, demonstrates antiviral efficacy against a wide range of viruses, including influenza A and B [16,17].

Remdesivir is an antiviral medicine that has been designed to help people avoid contracting the Ebola virus. As a nucleotide derivative drug, it hinders the replication of viral RNA [18,19].

Theaflavin is a natural catechin-based polymer wherein catechins are oxidized when plant leaves get dried. Two catechin molecules have been bonded in the C ring to produce theaflavins. Theaflavins are employed in cases where absorption (e.g., stomach ulcer, oral health) is not required [20,21].

Favipiravir is a nucleoside precursor that suppresses influenza virus strains across the range. It has a dose-dependent antiviral effect with nearly 100 percent oral bioavailability [22,23].

Being an effective second-generation protease inhibitor, Darunavir acts better against HIV-1. Darunavir was found to be one of the most promising hits for inhibiting the chymotrypsin-like protease of SARS-CoV2 by using computer-aided drug design approaches [24,25].

On November 26, 2021, WHO announced a new variant, B.1.1.529, called Omicron, as a variant of concern. Preliminary research suggests that Omicron may have a higher probability of reinfection than other variants of concern (i.e., those who have previously had COVID-19 may be more likely reinfected by Omicron). However, data is limited [26,27].

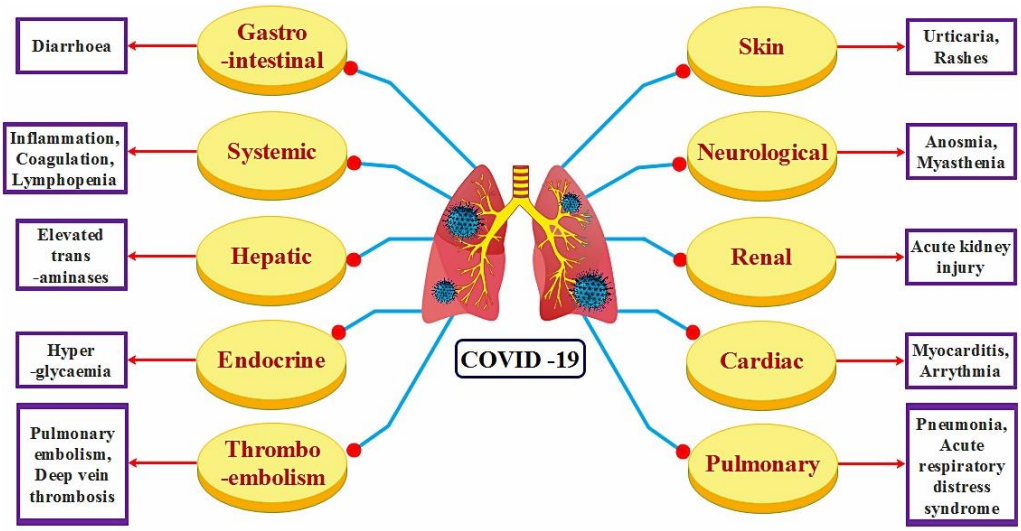

Figure 1. Certain manifestations related to COVID-19.

Recently, on December 22, 2021, Paxlovid and Molnupiravir were given Emergency Use Authorization (EUA) by the Food and Drug Administration (FDA) to treat mild-to-moderate COVID-19 in patients who are in danger of hospitalization or death. Paxlovid is a SARS-CoV-2 protease inhibitor antiviral, which contains two co-packaged drugs, Nirmatrelvir and Ritonavir [28,29]. As a direct-acting medication, Molnupiravir is the first oral antiviral that has been found to be highly effective in lowering nasopharyngeal SARS-CoV-2 infectious virus and viral RNA while also having a good therapeutic efficacy profile [30,31]. As of now, Paxlovid and Molnupiravir act effectively against omicron [32]. However, only limited information is available about the efficacy of using Paxlovid and Molnupiravir as they are investigational medicines. The chemical structures of certain drugs used to treat COVID-19 and Omicron are depicted in Figure 2 and Figure 3.

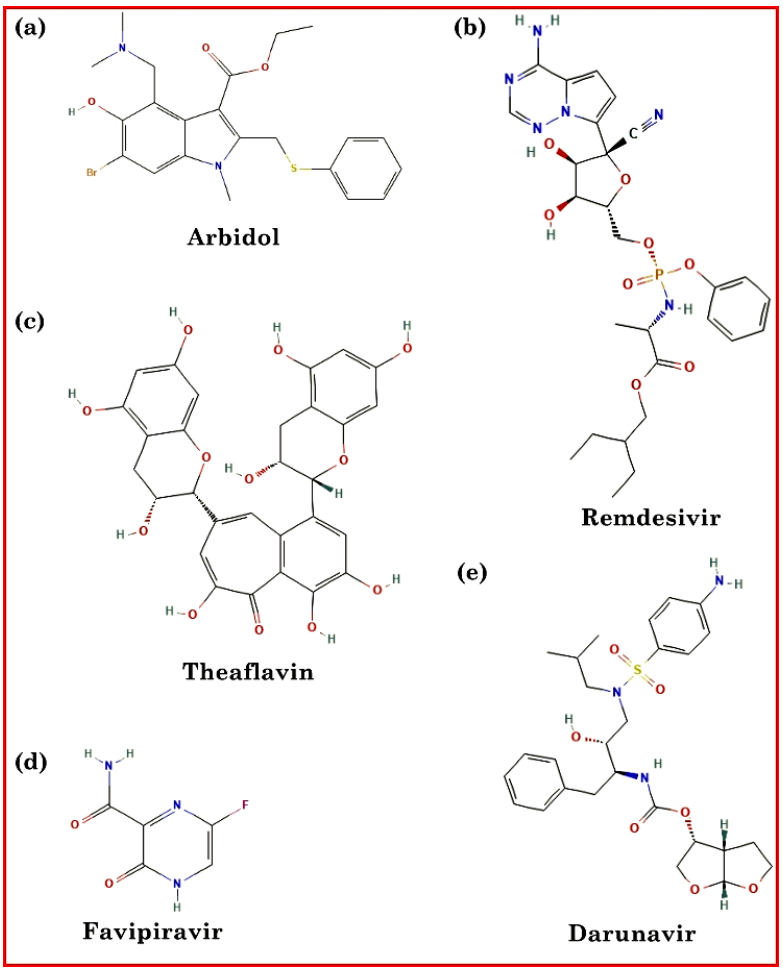

Figure 2. Chemical structure of **(a)** Arbidol; **(b)** Remdesivir; **(c)** Theaflavin; **(d)** Favipiravir; **(e)** Darunavir.

There have been numerous investigations on the aforementioned drugs and their derivatives are being conducted in an attempt to develop new medications for the therapies of COVID-19 disease [33-37]. Drugs are widely recognized as a critical tool for preventing and controlling disease. On the other hand, drug development is a time-consuming, complicated, and expensive procedure. This involves predicting the target substances' drug-likeness physicochemical and pharmacokinetic properties.

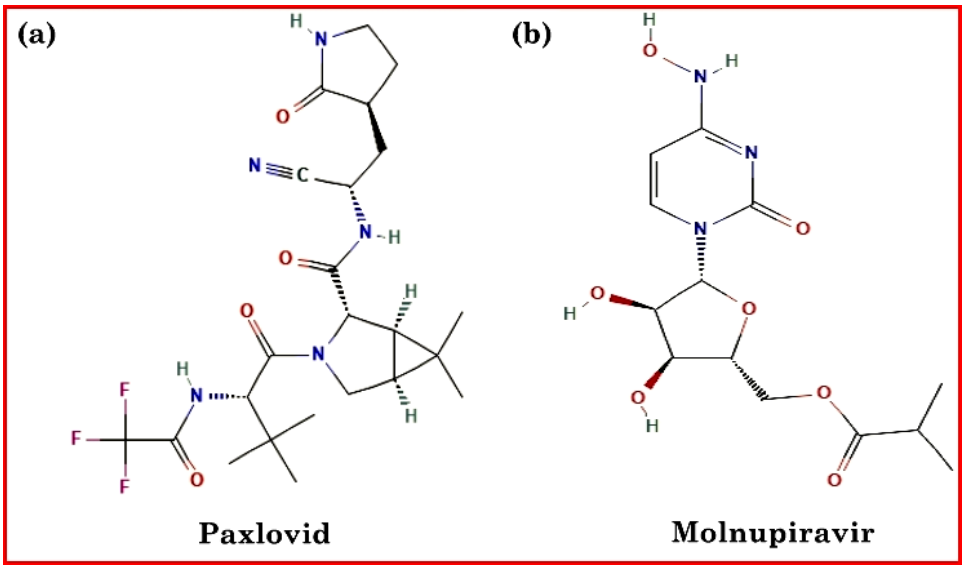

Figure 3. Chemical structure of **(a)** Paxlovid; **(b)** Molnupiravir.

1.1. Background.

Today, rapid advancements in mathematical chemistry have driven researchers to focus on making use of mathematical tools to achieve significant progress in several domains of chemistry, such as pharmaceutical sciences. Computational techniques for obtaining reliable analytical formulations for different TIs of diverse biological systems are the new advent of mathematical chemistry [38-41]. TIs are mathematical tools developed by graph theory for chemists to predict the physicochemical and biological behavior of molecular compounds, which also describe the topology of the molecular structure and remain unaltered under graph isomorphism [42-45].

The Wiener index was the first TI used in biology and chemistry in 1947 when chemist Wiener established it to investigate alkane boiling points [46]. Among the several classes of TIs, degree-based TIs have a strong ability to predict the physicochemical characteristics of chemical compounds [47]. The so-called degree-based TIs employed in mathematical chemistry are defined based on the degree of the node of a graph. For instance, the Zagreb index, developed by Gutman *et al.* [48], is among the most widely used TIs. A pair of hyper Zagreb indices were established by Shirdel *et al.* [49]. Furtula *et al.* [50] proposed the Forgotten index for analyzing the prediction potential of the physicochemical properties of certain chemicals. Further, the Randić [51], reciprocal Randić [52], Harmonic [53], atomic bond connectivity index [54], inverse sum [55], sum connectivity [56], symmetric division [57] indices were proposed by respective authors in their work. We recommend the literature [58-69] to the ambitious reader for some recent reports.

When dealing with diverse platforms of applied mathematics, especially in the realm of mathematical biology, graphing stands out as one of the most effective techniques for expressing and comprehending the topology of drugs/chemical compounds without employing quantum mechanics. The data contained in a graph can be encoded through various graph polynomials in graph theory [70-72]. Polynomials emerge in a number of different forms, including Pi polynomial, M-polynomial, and Hosoya polynomial [73-75]. Among them, the M-polynomial is the most generalized polynomial, which provides a great deal of information about graphs [76,77]. The topological indices are typically computed by employing definitions, while they can also be obtained using the derivatives and integrals on the graph's M-polynomials. Hence, if the graph has an M-polynomial, we may derive its various TIs. Different M-polynomials of various graphs have been proposed in recent years [78-81].

1.2. Proposed work

In this article, we introduce a set of novel node degree-based TIs, known as Lakvir indices, and discuss some of their core classifications. We exclusively consider simple, undirected, finite, and connected graphs throughout this study.

Let G = (V, E) be a chemical graph whose node set V (G) and link set E(G) represent a set of atoms and bonds, respectively. The number of nodes neighboring to *s* is the degree of a node $s \in V(G)$, represented by $d_G(s)$. Let N(w) be the neighborhood set of node *w*, which includes the neighbors of *w* [82-84].

The neighborhood degree-sum of a node $s \in V(G)$, is defined as

$$\delta_G(s) = \sum_{w \in N(s)} d_G(w) \qquad (1)$$

A clique of graph G is a complete subgraph of G, and the number of nodes in the largest clique is known as the clique number w of graph G [82-84].

In what follows, we define the Lakvir degree of a node $s \in V(G)$, $Lv_G(s) = \delta_G(s) + \omega$, and the node associated with the Lakvir degree is called the Lakvir node. The notation *sw* is the Lakvir link connecting the Lakvir nodes s and w.

First Lakvir index: $Lv1(G) = \sum_{sw \in E(G)} (Lv_G(s) + Lv_G(w))$ (2)

First Lakvir node index: $Lv1^*(G) = \sum_{s \in V(G)} Lv_G(s)^2$ (3)

Second Lakvir index: $Lv2(G) = \sum_{sw \in E(G)} (Lv_G(s)^2 + Lv_G(w)^2)$ (4)

Second Lakvir node index: $Lv2^*(G) = \sum_{s \in V(G)} Lv_G(s)^3$ (5)

Third Lakvir index: $Lv3(G) = \sum_{sw \in E(G)} (Lv_G(s)\, Lv_G(w))$ (6)

First hyper Lakvir index: $HLv1(G) = \sum_{sw \in E(G)} (Lv_G(s) + Lv_G(w))^2$ (7)

Second hyper Lakvir index: $HLv2(G) = \sum_{sw \in E(G)} (Lv_G(s)\ Lv_G(w))^2$ (8)

Fourth Lakvir index: $Lv4(G) = \sum_{sw \in E(G)} \frac{1}{\sqrt{Lv_G(s)\, Lv_G(w)}}$ (9)

Fifth Lakvir index: $Lv5(G) = \sum_{sw \in E(G)} \sqrt{Lv_G(s)\, Lv_G(w)}$ (10)

Lakvir sum connectivity index: $LvS(G) = \sum_{sw \in E(G)} \frac{1}{\sqrt{Lv_G(s) + Lv_G(w)}}$ (11)

Sixth Lakvir index: $Lv6(G) = \sum_{sw \in E(G)} Lv_G(s)\, Lv_G(w)\, (Lv_G(s) + Lv_G(w))$ (12)

Inverse Lakvir node index: $LvI(G) = \sum_{s \in V(G)} \frac{1}{Lv_G(s)}$ (13)

Lakvir symmetric division index: $LvSD(G) = \sum_{sw \in E(G)} \frac{Lv_G(s)^2 + Lv_G(w)^2}{Lv_G(s)\, Lv_G(w)}$ (14)

Lakvir inverse sum index: $LvISI(G) = \sum_{sw \in E(G)} \frac{Lv_G(s)\, Lv_G(w)}{Lv_G(s) + Lv_G(w)}$ (15)

Lakvir Harmonic index: $LvH(G) = \sum_{sw \in E(G)} \frac{2}{Lv_G(s) + Lv_G(w)}$ (16)

Lakvir atomic bond connectivity index:

$$LvABC(G) = \sum_{sw \in E(G)} \sqrt{\frac{Lv_G(s) + Lv_G(w) - 2}{Lv_G(s)\, Lv_G(w)}} \quad (17)$$

1.3. Preliminary investigations.

We employ statistical regression analysis, as recommended by the International Academy of Mathematical Chemistry, to determine the proposed TIs' effectiveness in predicting compounds' physiochemical behavior.

Linear Regression Model: $\xi = \nu + \mu(TI)$. (18)

Where ξ = Physical Property, TI = Topological Index, μ, and ν are constants.

Octane isomers are particularly useful for the preliminary investigation of indices as they represent a reasonably broad and structurally diverse group of alkanes. Herein, we focused on the novel indices for modeling physicochemical properties such as Boiling Points (BP), Entropy (S), Critical Pressure (PC), Mean Radius (R_m^2), Density (D), Heats of Vaporization ($-\Delta H_v$) at 25 °C Heats of Formation($-\Delta H_f$), Molar Volumes (MV) at 20°C, Acentric Factor (AF), Enthalpy of Vaporization (HVAP), Standard Enthalpy of Vaporization (DHVAP), and

Molar Refractions (MR) at 20 °C of octane isomers. We acquired the experimental data for the physicochemical properties of octane isomers from www.moleculardescriptors.eu.

Mathematically, the correlation coefficient (|R|) is calculated to evaluate how efficient a TI is in predicting the physicochemical properties of molecular compounds. QSPR/QSAR analysis prioritizes the TIs having significant |R| values (> 0.8). The novel TIs mentioned below have strong correlations with the AF (|R| = 0.991), S (|R| = 0.959), PC (|R| = 0.814), BP (|R| = 0.801), R_m^2 (|R| = 0.854), $-\Delta H_f$ (|R| = 0.881), MV (|R| = 0.941), MR (|R| = 0.971), HVAP (|R| =0.906), DHVAP (|R| = 0.912) of octane isomers (Table 1).

Table 1. Correlation of Lakvir indices with physicochemical properties of octane isomers.

	BP	S	PC	R_m^2	D	$-\Delta H_v$	$-\Delta H_f$	MV	AF	HVAP	DHVAP	MR
Lv1(G)	-0.498	-0.940	0.496	-0.816	0.728	-0.133	0.537	-0.614	-0.986	-0.726	-0.811	-0.675
Lv1*(G)	-0.658	-0.956	0.374	-0.805	0.664	-0.213	0.692	-0.378	-0.991	-0.847	-0.910	-0.449
Lv2(G)	-0.451	-0.931	0.512	-0.798	0.747	-0.099	0.492	-0.665	-0.978	-0.688	-0.779	-0.721
Lv2*(G)	-0.508	-0.804	0.269	-0.598	0.591	-0.111	0.591	-0.276	-0.820	-0.724	-0.740	-0.318
Lv3(G)	-0.499	-0.945	0.473	-0.797	0.743	-0.110	0.544	-0.608	-0.986	-0.724	-0.812	-0.667
HLv1(G)	-0.473	-0.938	0.494	-0.798	0.745	-0.104	0.516	-0.639	-0.982	-0.705	-0.795	-0.696
HLv2(G)	-0.446	-0.937	0.475	-0.763	0.771	-0.060	0.500	-0.659	-0.976	-0.681	-0.776	-0.712
Lv4(G)	0.585	0.949	-0.459	0.852	-0.683	0.197	-0.620	0.506	0.991	0.795	0.865	0.576
Lv5(G)	-0.528	-0.948	0.469	-0.815	0.726	-0.138	0.569	-0.577	-0.989	-0.747	-0.830	-0.639
LvS(G)	0.537	0.942	-0.498	0.844	-0.697	0.178	-0.571	0.572	0.989	0.758	0.836	0.638
Lv6(G)	-0.464	-0.939	0.480	-0.780	0.759	-0.082	0.513	-0.644	-0.980	-0.696	-0.789	-0.699
LvI(G)	0.801	0.853	-0.139	0.667	-0.468	0.287	-0.881	-0.058	0.839	0.906	0.912	-0.002
LvSD(G)	0.043	-0.600	0.814	-0.647	0.557	-0.073	-0.044	-0.941	-0.710	-0.239	-0.349	-0.971
LvISI(G)	-0.559	-0.955	0.438	-0.812	0.722	-0.143	0.603	-0.533	-0.991	-0.770	-0.850	-0.597
LvH(G)	0.549	0.941	-0.498	0.854	-0.686	0.194	-0.582	0.556	0.989	0.768	0.844	0.624
LvABC(G)	0.615	0.959	-0.399	0.827	-0.698	0.173	-0.657	0.452	0.989	0.813	0.882	0.521

The purpose of TI is to figure out as much as possible about the structural properties of a compound. A robust topological descriptor should have been capable of distinguishing the various structural formulae. With a high discriminating power, TIs can obtain more structural information. Degeneracy is a major flaw in TIs that occurs when two or more isomers have the same TI. An associated concern in this respect is finding new topological indices with high discriminating power to characterize the structure of such isomer chemical graphs uniquely. For this objective, we propose a set of novel node degree-based TIs, known as Lakvir indices, and further employed Konstantinova's sensitivity [85] as a measure of degeneracy, which is defined below,

$$S_I = \frac{H - H_I}{H} \quad (19)$$

Where H represents the total number of isomers examined, and H_I denotes the number of isomers that the TI I cannot differentiate. The isomer-discrimination capacity of TIs grows in accordance with S_I. Unambiguously, the highest value of S_I is 1. The newly proposed Lakvir indices outperform certain well-established degree-based indices and exhibit superior discriminating power (the value of S_I is exactly 1) to octane isomers (Table 2).

Having high statistical accuracy, it is worthwhile to compute these novel indices for various clinically significant drugs. At this juncture of the research, we compute these indices

via LM polynomials towards some drugs used to treat COVID-19 and Omicron to disclose their mathematical behavior.

Table 2. The measure of sensitivity (S_I) of various indices for octane isomers.

TI	Sensitivity (S_I)
Lv1*(G)	**1.000**
Lv2(G)	**1.000**
Lv2*(G)	**1.000**
Lv3(G)	**1.000**
HLv1(G)	**1.000**
HLv2(G)	**1.000**
Lv4(G)	**1.000**
Lv5(G)	**1.000**
LvS(G)	**1.000**
Lv6(G)	**1.000**
LvI(G)	**1.000**
LvSD(G)	**1.000**
LvISI(G)	**1.000**
LvH(G)	**1.000**
LvABC(G)	**1.000**
Lv1(G)	**0.722**
Merrifield - Simmons index	0.833
Hyper Zagreb index	0.833
Hosoya index Z	0.778
Second Zagreb index $M_2(G)$	0.722
Forgotten Index F(G)	0.389
First Zagreb index $M_1(G)$	0.333

2. Materials and Methods

The chemical structure of the considered drugs can be accessed at pubchem.ncbi.nlm.nih.gov. Consider a hydrogen-suppressed chemical graph of a drug since the vertices representing hydrogen atoms do not contribute to graph isomorphism. To obtain our main results, we employed statistical methods, graph-theoretical terminologies, combinatorial computation, analytic approaches, node and edge partition techniques, and methods of counting degrees.

Throughout this article, the symbols V_α and $E_{(\beta,\gamma)}$ are designated for node and edge partitions, respectively.

$$V_\alpha = \{s \in V(G) : Lv_G(s) = \alpha\}, \quad (20)$$

$$E_{(\beta,\gamma)} = \{sw \in E(G) : Lv_G(s) = \beta, Lv_G(w) = \gamma\}. \quad (21)$$

2.1. Theorem[86]

Let G be a simple connected graph.

If $S(G) = \sum_{uv \in E(G)} \Lambda(d(u), d(v))$, where $\Lambda(x, y)$ is a polynomial in x and y, then $S(G) = \Lambda(D_x, D_y)(M(G; x, y))|_{x=y=1}$.

$If\ S(G) = \sum_{u\,v\,\in E(G)} \Lambda\left(\mathrm{d}(u), d(v)\right)$, where $\Lambda(x,y) = \sum_{i,j\in\mathbb{Z}} \varepsilon_{i,j}\, x^{i} y^{\mathrm{j}}$ then S(G) can be obtained by $M(G;\, x, y)$ using the operators D_x, D_y, I_x, I_y.

$If\ S(G) = \sum_{u\,v\,\in E(G)} \Lambda\left(\mathrm{d}(u), d(v)\right)$, where $\Lambda(x,y) = \frac{x^{\mathrm{r}}\, y^{s}}{(x+y+\vartheta)^{t}}$, where $\mathrm{r}, \mathrm{s} \geq 0, \mathrm{t} \geq 1$ and $\vartheta \in \mathbb{Z}$, then $S(G) = I_x^{\mathrm{t}}\, Q_{\vartheta} J D_{\mathrm{x}}^{\mathrm{r}} D_{\mathrm{y}}^{\mathrm{s}}\ (M(G;\, x, y))|_{x=y=1}$.

In a similar fashion, the LM Polynomial of a chemical graph is defined as,

$$LM(G;\, x, y) = \sum_{\beta \leq \gamma} \left(\begin{array}{c}\text{Number of every edges } s \text{ w such that} \\ Lv_G(s) = \beta, Lv_G(w) = \gamma\end{array}\right) x^{\beta}\, y^{\gamma} \qquad (22)$$

$$D_x = x\, \frac{\partial(\Lambda(x,y))}{\partial x},\ D_y = y\, \frac{\partial(\Lambda(x,y))}{\partial y},\ I_x = \int_0^x \frac{\Lambda(t,y)}{t}\, dt,\ I_y = \int_0^y \frac{\Lambda(x,t)}{t}\, dt,$$
$$J(\Lambda(x,y)) = \Lambda(x,x) \text{ and } Q_{\vartheta}(\Lambda(x,y)) = x^{\vartheta}\Lambda(x,y),\ \vartheta \neq 0. \qquad (23)$$

To assess the considered TIs (as given in Table 3) of a graph G from the LM(G; x, y), the formulae of derivations in terms of derivative or integral (or both integral and derivative) are employed. Where:

The node, edge cardinality, and node partition of the considered drugs are displayed in Table 4 and Table 5, respectively.

The edge partition and the cardinality of the drugs are as follows,

(i) For Arbidol:

$$E(G) = E_{(4,5)} \cup E_{(5,6)} \cup E_{(5,7)} \cup E_{(5,8)} \cup E_{(5,9)} \cup E_{(6,6)} \cup E_{(6,7)} \cup E_{(6,8)} \cup E_{(7,7)} \cup E_{(7,8)} \cup E_{(7,10)} \cup E_{(8,8)} \cup E_{(8,9)} \cup E_{(8,10)} \cup E_{(8,11)} \cup E_{(9,10)} \cup E_{(10,11)} \cup E_{(11,11)}.$$

$$|E_{(4,5)}| = 1;\ |E_{(5,6)}| = 2;\ |E_{(5,7)}| = 1;\ |E_{(5,8)}| = 2;\ |E_{(5,9)}| = 2;\ |E_{(6,6)}| = 2;\ |E_{(6,7)}| = 2;\ |E_{(6,8)}| = 1;\ |E_{(7,7)}| = 1;\ |E_{(7,8)}| = 4;\ |E_{(7,10)}| = 1;\ |E_{(8,8)}| = 1;\ |E_{(8,9)}| = 1;\ |E_{(8,10)}| = 1;\ |E_{(8,11)}| = 2;\ |E_{(9,10)}| = 3;\ |E_{(10,11)}| = 3;\ |E_{(11,11)}| = 1.$$

(ii) For Remdesivir:

$$E(G) = E_{(4,6)} \cup E_{(4,7)} \cup E_{(5,8)} \cup E_{(5,9)} \cup E_{(5,10)} \cup E_{(6,6)} \cup E_{(6,7)} \cup E_{(6,8)} \cup E_{(6,9)} \cup E_{(7,7)} \cup E_{(7,8)} \cup E_{(7,9)} \cup E_{(7,10)} \cup E_{(7,11)} \cup E_{(7,12)} \cup E_{(8,8)} \cup E_{(8,9)} \cup E_{(8,10)} \cup E_{(9,9)} \cup E_{(9,10)} \cup E_{(9,12)} \cup E_{(10,10)} \cup E_{(10,11)} \cup E_{(10,12)} \cup E_{(11,12)}.$$

$$|E_{(4,6)}| = 2;\ |E_{(4,7)}| = 1;\ |E_{(5,8)}| = 3;\ |E_{(5,9)}| = 1;\ |E_{(5,10)}| = 1;\ |E_{(6,6)}| = 2;\ |E_{(6,7)}| = 4;\ |E_{(6,8)}| = 2;\ |E_{(6,9)}| = 1;\ |E_{(7,7)}| = 2;\ |E_{(7,8)}| = 6;\ |E_{(7,9)}| = 1;\ |E_{(7,10)}| = 2;\ |E_{(7,11)}| = 1;\ |E_{(7,12)}| = 1;\ |E_{(8,8)}| = 1;\ |E_{(8,9)}| = 3;\ |E_{(8,10)}| = 1;\ |E_{(9,9)}| = 4;\ |E_{(9,10)}| = 1;\ |E_{(9,12)}| = 1;\ |E_{(10,10)}| = 1;\ |E_{(10,11)}| = 1;\ |E_{(10,12)}| = 1;\ |E_{(11,12)}| = 1.$$

(iii) For Theaflavin:

$$E(G) = E_{(5,7)} \cup E_{(5,8)} \cup E_{(5,9)} \cup E_{(7,8)} \cup E_{(8,8)} \cup E_{(8,9)} \cup E_{(8,10)} \cup E_{(9,10)} \cup E_{(9,11)} \cup E_{(10,10)} \cup E_{(10,11)}.$$

$$|E_{(5,7)}| = 2;\ |E_{(5,8)}| = 6;\ |E_{(5,9)}| = 2;\ |E_{(7,8)}| = 4;\ |E_{(8,8)}| = 6;\ |E_{(8,9)}| = 8;\ |E_{(8,10)}| = 10;\ |E_{(9,10)}| = 3;\ |E_{(9,11)}| = 2;\ |E_{(10,10)}| = 2;\ |E_{(10,11)}| = 1.$$

(iv) For Favipiravir:

$$E(G) = E_{(5,7)} \cup E_{(5,8)} \cup E_{(7,7)} \cup E_{(7,8)} \cup E_{(7,10)} \cup E_{(8,10)}.$$
$$|E_{(5,7)}| = 3; |E_{(5,8)}| = 1; |E_{(7,7)}| = 2; |E_{(7,8)}| = 2; |E_{(7,10)}| = 1; |E_{(8,10)}| = 2.$$

(v) For Darunavir:

$$E(G) = E_{(5,6)} \cup E_{(5,7)} \cup E_{(5,8)} \cup E_{(6,6)} \cup E_{(6,7)} \cup E_{(6,8)} \cup E_{(6,10)} \cup E_{(7,7)} \cup E_{(7,8)} \cup E_{(7,9)} \cup E_{(7,10)} \cup E_{(8,8)} \cup E_{(8,9)} \cup E_{(8,10)} \cup E_{(9,10)} \cup E_{(10,10)}.$$

$$|E_{(5,6)}| = 2; |E_{(5,7)}| = 2; |E_{(5,8)}| = 1; |E_{(6,6)}| = 2; |E_{(6,7)}| = 4; |E_{(6,8)}| = 1;$$
$$|E_{(6,10)}| = 2; |E_{(7,7)}| = 5; |E_{(7,8)}| = 4; |E_{(7,9)}| = 3; |E_{(7,10)}| = 3;$$
$$|E_{(8,8)}| = 2; |E_{(8,9)}| = 4; |E_{(8,10)}| = 2; |E_{(9,10)}| = 2; |E_{(10,10)}| = 2.$$

(vi) For Paxlovid:

$$E(G) = E_{(5,7)} \cup E_{(6,9)} \cup E_{(6,10)} \cup E_{(7,8)} \cup E_{(7,9)} \cup E_{(7,11)} \cup E_{(8,9)} \cup E_{(8,10)} \cup E_{(9,9)} \cup E_{(9,10)} \cup E_{(9,11)} \cup E_{(9,12)} \cup E_{(10,11)} \cup E_{(10,12)} \cup E_{(11,12)} \cup E_{(11,13)} \cup E_{(12,13)}.$$

$$|E_{(5,7)}| = 1; |E_{(6,9)}| = 2; |E_{(6,10)}| = 2; |E_{(7,8)}| = 2; |E_{(7,9)}| = 7; |E_{(7,11)}| = 2;$$
$$|E_{(8,9)}| = 1; |E_{(8,10)}| = 1; |E_{(9,9)}| = 3; |E_{(9,10)}| = 4; |E_{(9,11)}| = 1;$$
$$|E_{(9,12)}| = 4; |E_{(10,11)}| = 1; |E_{(10,12)}| = 1; |E_{(11,12)}| = 2; |E_{(11,13)}| = 1;$$
$$|E_{(12,13)}| = 2.$$

(vii) For Molnupiravir:

$$E(G) = E_{(4,6)} \cup E_{(5,7)} \cup E_{(5,8)} \cup E_{(5,9)} \cup E_{(6,8)} \cup E_{(7,7)} \cup E_{(7,8)} \cup E_{(7,9)} \cup E_{(7,10)} \cup E_{(8,8)} \cup E_{(8,9)} \cup E_{(8,10)} \cup E_{(9,9)} \cup E_{(9,10)} \cup E_{(10,10)}.$$

$$|E_{(4,6)}| = 1; |E_{(5,7)}| = 2; |E_{(5,8)}| = 2; |E_{(5,9)}| = 2; |E_{(6,8)}| = 1; |E_{(7,7)}| = 2;$$
$$|E_{(7,8)}| = 3; |E_{(7,9)}| = 1; |E_{(7,10)}| = 1; |E_{(8,8)}| = 2; |E_{(8,9)}| = 1;$$
$$|E_{(8,10)}| = 2; |E_{(9,9)}| = 2; |E_{(9,10)}| = 1; |E_{(10,10)}| = 1.$$

Table 3. Degree-based TIs are derived from the LM Polynomial of graph G.

S. No.	TI	$\Lambda(x,y)$	Derivation from $LM(G;x,y)$
1.	$Lv1(G)$	$x+y$	$(D_x + D_y)\ (LM(G;x,y))\|_{x=y=1}$
2.	$Lv2(G)$	x^2+y^2	$(D_x^2 + D_y^2)\ (LM(G;x,y))\|_{x=y=1}$
3.	$Lv3(G)$	xy	$(D_xD_y)\ (LM(G;x,y))\|_{x=y=1}$
4.	$Lv4(G)$	$\frac{1}{\sqrt{xy}}$	$(D_x^{\frac{-1}{2}} D_y^{\frac{-1}{2}})\ (LM(G;x,y))\|_{x=y=1}$
5.	$Lv5(G)$	$\sqrt{xy}$	$(D_x^{\frac{1}{2}} D_y^{\frac{1}{2}})\ (LM(G;x,y))\|_{x=y=1}$
6.	$LvS(G)$	$\frac{1}{\sqrt{x+y}}$	$I_x^{\frac{1}{2}} J\ (LM(G;x,y))\|_{x=1}$
7.	$Lv6(G)$	$xy(x+y)$	$D_x D_y(D_x + D_y)\ (LM(G;x,y))\|_{x=y=1}$
8.	$LvSD(G)$	$\frac{x^2+y^2}{xy}$	$(D_xI_y + D_yI_x)\ (LM(G;x,y))\|_{x=y=1}$
9.	$LvISI(G)$	$\frac{xy}{x+y}$	$I_x J\ D_xD_y\ (LM(G;x,y))\|_{x=1}$
10.	$LvH(G)$	$\frac{2}{x+y}$	$2\ I_x J\ (LM(G;x,y))\|_{x=1}$
11.	$LvABC(G)$	$\sqrt{\frac{x+y-2}{xy}}$	$I_x^{\frac{-1}{2}} Q_{-2} J D_x^{\frac{-1}{2}} D_y^{\frac{-1}{2}}\ (LM(G;x,y))\|_{x=1}$
12.	$HLv1(G)$	$(x+y)^2$	$(D_x^2 + D_y^2 + 2D_xD_y)(LM(G;x,y))\|_{x=y=1}$

S. No.	TI	$\Lambda(x,y)$	Derivation from $LM(G;x,y)$
13.	$HLv2(G)$	$(xy)^2$	$(D_xD_y)(D_xD_y)\ (LM(G;x,y))\vert_{x=y=1}$

Table 4. Associated drugs with node and edge cardinality.

S. No.	Drug with chemical formula	Node cardinality	Edge cardinality
1.	Arbidol ($C_{22}H_{25}BrN_2O_3S$)	29	31
2.	Remdesivir ($C_{27}H_{35}N_6O_8P$)	42	45
3.	Theaflavin ($C_{29}H_{24}O_{12}$)	41	46
4.	Favipiravir($C_5H_4FN_3O_2$)	11	11
5.	Darunavir ($C_{27}H_{37}N_3O_7S$)	38	41
6.	Paxlovid (Nirmatrelvir) ($C_{23}H_{32}F_3N_5O_4$)	35	37
7.	Molnupiravir ($C_{13}H_{19}N_3O_7$)	23	24

Table 5. Associated drugs with node partition.

Drug	Node partition								
Arbidol	$V(G)=V_4\cup V_5\cup V_6\cup V_7\cup V_8\cup V_9\cup V_{10}\cup V_{11}$								
	V_α	V_4	V_5	V_6	V_7	V_8	V_9	V_{10}	V_{11}
	$\vert V_\alpha \vert$	1	7	4	5	5	2	3	2
Remdesivir	$V(G)=V_4\cup V_5\cup V_6\cup V_7\cup V_8\cup V_9\cup V_{10}\cup V_{11}\cup V_{12}$								
	V_α	V_4	V_5	V_6	V_7	V_8	V_9	V_{10}	V_{11}	V_{12}
	$\vert V_\alpha \vert$	3	5	7	10	6	6	3	1	1
Theaflavin	$V(G)=V_5\cup V_7\cup V_8\cup V_9\cup V_{10}\cup V_{11}$								
	V_α	V_5	V_7	V_8	V_9	V_{10}	V_{11}		
	$\vert V_\alpha \vert$	10	2	17	4	7	1		
Favipiravir	$V(G)=V_5\cup V_7\cup V_8\cup V_{10}$								
	V_α	V_5	V_7	V_8	V_{10}				
	$\vert V_\alpha \vert$	4	4	2	1				
Darunavir	$V(G)=V_5\cup V_6\cup V_7\cup V_8\cup V_9\cup V_{10}$								
	V_α	V_5	V_6	V_7	V_8	V_9	V_{10}		
	$\vert V_\alpha \vert$	5	7	12	7	3	4		
Paxlovid (Nirmatrelvir)	$V(G)=V_5\cup V_6\cup V_7\cup V_8\cup V_9\cup V_{10}\cup V_{11}\cup V_{12}\cup V_{13}$								
	V_α	V_5	V_6	V_7	V_8	V_9	V_{10}	V_{11}	V_{12}	V_{13}
	$\vert V_\alpha \vert$	1	4	10	2	9	3	2	3	1
Molnupiravir	$V(G)=V_4\cup V_5\cup V_6\cup V_7\cup V_8\cup V_9\cup V_{10}$								
	V_α	V_4	V_5	V_6	V_7	V_8	V_9	V_{10}		
	$\vert V_\alpha \vert$	1	6	1	5	5	3	2		

3. Results and Discussion

The main computational results are presented in this section.

Lemma 3.1.

If G is a molecular graph of the Arbidol drug, then:

$$LM(G;\,x,y) = x^4y^5 + 2x^5y^6 + x^5y^7 + 2x^5y^8 + 2x^5y^9 + 2x^6y^6 + 2x^6y^7 + x^6y^8 + x^7y^7 + 4x^7y^8 + x^7y^{10} + x^8y^8 + x^8y^9 + x^8y^{10} + 2x^8y^{11} + 3x^9y^{10} + 3x^{10}y^{11} + x^{11}y^{11}.$$

Proof:

From equation (22), The LM Polynomial of G arrives as follows.

$$LM(G;x,y) = \sum_{\beta \le \gamma} |E_{(\beta,\gamma)}|\, x^\beta y^\gamma = |E_{(4,5)}|x^4y^5 + |E_{(5,6)}|x^5y^6 + |E_{(5,7)}|x^5y^7 + |E_{(5,8)}|x^5y^8 + |E_{(5,9)}|x^5y^9 + |E_{(6,6)}|x^6y^6 + |E_{(6,7)}|x^6y^7 + |E_{(6,8)}|x^6y^8 + |E_{(7,7)}|x^7y^7 + |E_{(7,8)}|x^7y^8 + |E_{(7,10)}|x^7y^{10} + |E_{(8,8)}|x^8y^8 + |E_{(8,9)}|x^8y^9 + |E_{(8,10)}|x^8y^{10} + |E_{(8,11)}|x^8y^{11} + |E_{(9,10)}|x^9y^{10} + |E_{(10,11)}|x^{10}y^{11} + |E_{(11,11)}|x^{11}y^{11}.$$

$$= x^4y^5 + 2x^5y^6 + x^5y^7 + 2x^5y^8 + 2x^5y^9 + 2x^6y^6 + 2x^6y^7 + x^6y^8 + x^7y^7 + 4x^7y^8 + x^7y^{10} + x^8y^8 + x^8y^9 + x^8y^{10} + 2x^8y^{11} + 3x^9y^{10} + 3x^{10}y^{11} + x^{11}y^{11}.$$

Now, we evaluate some Lakvir TIs for the molecular graph of Arbidol using LM Polynomials derived in Lemma 3.1.

Theorem 3.1.

Let G be a chemical graph of the Arbidol drug. Then, we have:

(i) $Lv1(G)$= 483. (ii) $Lv2(G)$=3633. (iii) $Lv3(G)$ = 1945.

(iv) $Lv4(G)$= 4.215. (v) $Lv5(G)$ = 246.65. (vi) $LvS(G)$= 7.97.

(vii) $Lv6(G)$= 33178. (viii) $LvSD(G)$ = 64.04. (ix) $LvISI(G)$= 118.96.

(x) $LvH(G)$= 4.165. (xi) $LvABC(G)$= 14.96. (xii) $HLv1(G)$ = 7885.

(xiii) $HLv2(G)$= 145353.

Proof:

Consider the LM Polynomial of Arbidol,

$$LM(G;\,x,y) = x^4y^5 + 2x^5y^6 + x^5y^7 + 2x^5y^8 + 2x^5y^9 + 2x^6y^6 + 2x^6y^7 + x^6y^8 + x^7y^7 + 4x^7y^8 + x^7y^{10} + x^8y^8 + x^8y^9 + x^8y^{10} + 2x^8y^{11} + 3x^9y^{10} + 3x^{10}y^{11} + x^{11}y^{11}.$$

$$(D_x + D_y)(\Lambda(x,y)) = 9x^4y^5 + 22x^5y^6 + 12x^5y^7 + 26x^5y^8 + 28x^5y^9 + 24x^6y^6 + 26x^6y^7 + 14x^6y^8 + 14x^7y^7 + 60x^7y^8 + 17x^7y^{10} + 16x^8y^8 + 17x^8y^9 + 18x^8y^{10} + 38x^8y^{11} + 57x^9y^{10} + 63x^{10}y^{11} + 22x^{11}y^{11}.$$

$$(D_x^2 + D_y^2)(\Lambda(x,y)) = 41x^4y^5 + 122x^5y^6 + 74x^5y^7 + 178x^5y^8 + 212x^5y^9 + 144x^6y^6 + 170x^6y^7 + 100x^6y^8 + 98x^7y^7 + 452x^7y^8 + 149x^7y^{10} + 128x^8y^8 + 145x^8y^9 + 164x^8y^{10} + 370x^8y^{11} + 181x^9y^{10} + 663x^{10}y^{11} + 242x^{11}y^{11}.$$

$$(D_x D_y)(\Lambda(x,y)) = 20x^4y^5 + 60x^5y^6 + 35x^5y^7 + 80x^5y^8 + 90x^5y^9 + 72x^6y^6 + 84x^6y^7 + 48x^6y^8 + 49x^7y^7 + 224x^7y^8 + 70x^7y^{10} + 64x^8y^8 + 72x^8y^9 + 80x^8y^{10} + 176x^8y^{11} + 270x^9y^{10} + 330x^{10}y^{11} + 121x^{11}y^{11}.$$

$$(D_x D_y)(D_x D_y)(\Lambda(x,y)) = 400x^4y^5 + 1800x^5y^6 + 1225x^5y^7 + 3200x^5y^8 + 4050x^5y^9 + 2592x^6y^6 + 3528x^6y^7 + 2304x^6y^8 + 2401x^7y^7 + 12544x^7y^8 + 4900x^7y^{10} + 4096x^8y^8 + 5184x^8y^9 + 6400x^8y^{10} + 15488x^8y^{11} + 24300x^9y^{10} + 36300x^{10}y^{11} + 14641x^{11}y^{11}.$$

$$(D_x^{\frac{1}{2}} D_y^{\frac{1}{2}})(\Lambda(x,y)) = 4.47x^4y^5 + 10.95x^5y^6 + 5.92x^5y^7 + 12.65x^5y^8 + 13.42x^5y^9 + 12x^6y^6 + 12.96x^6y^7 + 13.86x^6y^8 + 7x^7y^7 + 29.9x^7y^8 + 8.37x^7y^{10} + 8x^8y^8 + 8.49x^8y^9 + 8.94x^8y^{10} + 18.76x^8y^{11} + 28.5x^9y^{10} + 31.46x^{10}y^{11} + 11x^{11}y^{11}.$$

$$(D_x^{\frac{-1}{2}} D_y^{\frac{-1}{2}})(\Lambda(x,y)) = 0.22x^4y^5 + 0.37x^5y^6 + 0.17x^5y^7 + 0.32x^5y^8 + 0.3x^5y^9 + 0.33x^6y^6 + 0.31x^6y^7 + 0.14x^6y^8 + 0.14x^7y^7 + 0.53x^7y^8 + 0.12x^7y^{10} + 0.125x^8y^8 + 0.12x^8y^9 + 0.11x^8y^{10} + 0.21x^8y^{11} + 0.32x^9y^{10} + 0.29x^{10}y^{11} + 0.09x^{11}y^{11}.$$

$$J(\Lambda(x,y)) = x^9 + 2x^{11} + 3x^{12} + 4x^{13} + 4x^{14} + 4x^{15} + x^{16} + 2x^{17} + x^{18} + 5x^{19} + 3x^{21} + x^{22}.$$

$$I_x^{\frac{1}{2}} J(\Lambda(x,y)) = 0.3x^9 + 0.6x^{11} + 0.87x^{12} + 1.11x^{13} + 1.07x^{14} + 1.03x^{15} + 0.25x^{16} + 0.49x^{17} + 0.24x^{18} + 1.15x^{19} + 0.65x^{21} + 0.21x^{22}.$$

$$I_x J(\Lambda(x,y)) = \frac{1}{9}x^9 + \frac{2}{11}x^{11} + \frac{3}{12}x^{12} + \frac{4}{13}x^{13} + \frac{4}{14}x^{14} + \frac{4}{15}x^{15} + \frac{1}{16}x^{16} + \frac{2}{17}x^{17} + \frac{1}{18}x^{18} + \frac{5}{19}x^{19} + \frac{3}{21}x^{21} + \frac{1}{22}x^{22}.$$

$$2I_x J(\Lambda(x,y)) = 0.2x^9 + 0.36x^{11} + 0.5x^{12} + 0.62x^{13} + 0.57x^{14} + 0.53x^{15} + 0.125x^{16} + 0.24x^{17} + 0.11x^{18} + 0.53x^{19} + 0.29x^{21} + 0.09x^{22}.$$

$$J(D_x D_y)(\Lambda(x,y)) = 20x^9 + 60x^{11} + 107x^{12} + 164x^{13} + 187x^{14} + 224x^{15} + 64x^{16} + 142x^{17} + 80x^{18} + 446x^{19} + 330x^{21} + 121x^{22}.$$

$$I_x J(D_x D_y)(\Lambda(x,y)) = 2.22x^9 + 5.45x^{11} + 8.92x^{12} + 12.61x^{13} + 13.36x^{14} + 14.93x^{15} + 4x^{16} + 8.35x^{17} + 4.44x^{18} + 23.47x^{19} + 15.71x^{21} + 5.5x^{22}.$$

$$(D_x D_y)(D_x + D_y)(\Lambda(x,y)) = 180x^4y^5 + 660x^5y^6 + 420x^5y^7 + 1040x^5y^8 + 1260x^5y^9 + 864x^6y^6 + 1092x^6y^7 + 672x^6y^8 + 686x^7y^7 + 3360x^7y^8 + 1190x^7y^{10} + 1024x^8y^8 + 1224x^8y^9 + 1440x^8y^{10} + 3344x^8y^{11} + 5130x^9y^{10} + 6930x^{10}y^{11} + 2662x^{11}y^{11}.$$

$$(D_x I_y + D_y I_x)(\Lambda(x,y)) = 2.05x^4y^5 + 4.07x^5y^6 + 2.11x^5y^7 + 4.45x^5y^8 + 4.71x^5y^9 + 4x^6y^6 + 4.05x^6y^7 + 2.08x^6y^8 + 2x^7y^7 + 8.07x^7y^8 + 2.13x^7y^{10} + 2x^8y^8 + 2.01x^8y^9 + 2.05x^8y^{10} + 4.2x^8y^{11} + 6.03x^9y^{10} + 6.03x^{10}y^{11} + 2x^{11}y^{11}.$$

$$(D_x^2 + D_y^2 + 2D_x D_y)(\Lambda(x,y)) = 81x^4y^5 + 242x^5y^6 + 144x^5y^7 + 338x^5y^8 + 392x^5y^9 + 288x^6y^6 + 338x^6y^7 + 196x^6y^8 + 196x^7y^7 + 900x^7y^8 + 289x^7y^{10} + 256x^8y^8 + 289x^8y^9 + 324x^8y^{10} + 722x^8y^{11} + 1083x^9y^{10} + 1323x^{10}y^{11} + 484x^{11}y^{11}.$$

$$(I_x^{\frac{-1}{2}} Q_{-2} J D_x^{\frac{-1}{2}} D_y^{\frac{-1}{2}})(\Lambda(x,y)) = 0.58x^7 + 1.11x^9 + 1.58x^{10} + 2.09x^{11} + 2x^{12} + 1.91x^{13} + 0.47x^{14} + 0.93x^{15} + 0.44x^{16} + 2.19x^{17} + 1.26x^{19} + 0.4x^{20}.$$

Using Table 3 and the above expressions, one can get:

(i) $Lv1(G) = (D_x + D_y)\ (LM(G;x,y))|_{x=y=1} = 483.$

(ii) $Lv2(G) = (D_x^2 + D_y^2)\ (LM(G;x,y))|_{x=y=1} = 3633.$

(iii) $Lv3(G) = (D_x D_y)\ (LM(G;x,y))|_{x=y=1} = 1945.$

(iv) $Lv4(G) = (D_x^{\frac{-1}{2}} D_y^{\frac{-1}{2}})\ (LM(G;x,y))|_{x=y=1} = 4.215.$

(v) $Lv5(G) = (D_x^{\frac{1}{2}} D_y^{\frac{1}{2}})\ (LM(G;x,y))|_{x=y=1} = 246.65.$

(vi) $LvS(G) = I_x^{\frac{1}{2}} J\ (LM(G;x,y))|_{x=1} = 7.97.$

(vii) $Lv6(G) = D_x D_y (D_x + D_y)\ (LM(G;x,y))|_{x=y=1} = 33178.$

(viii) $LvSD(G) = (D_x I_y + D_y I_x)\ (LM(G;x,y))|_{x=y=1} = 64.04.$

(ix) $LvISI(G) = I_x J D_x D_y\ (LM(G;x,y))|_{x=1} = 118.96.$

(x) $LvH(G) = 2\ I_x J\ (LM(G;x,y))|_{x=1} = 4.165.$

(xi) $LvABC(G) = I_x^{\frac{-1}{2}} Q_{-2} JD_x^{\frac{-1}{2}} D_y^{\frac{-1}{2}} (LM(G;x,y))|_{x=1}$ =14.96.

(xii) $HLv1(G) = (D_x^2 + D_y^2 + 2D_xD_y)(LM(G;x,y))|_{x=y=1}$ =7885.

(xiii) $HLv2(G) = (D_xD_y)(D_xD_y)\ (LM(G;x,y))|_{x=y=1}$ =145353.

Lemma 3.2.

If G is a molecular graph of the Remdesivir drug, then:

$$LM(G;x,y) = 2x^4y^6 + x^4y^7 + 3x^5y^8 + x^5y^9 + x^5y^{10} + 2x^6y^6 + 4x^6y^7 + 2x^6y^8 + x^6y^9 + 2x^7y^7 + 6x^7y^8 + x^7y^9 + 2x^7y^{10} + x^7y^{11} + x^7y^{12} + x^8y^8 + 3x^8y^9 + x^8y^{10} + 4x^9y^9 + x^9y^{10} + x^9y^{12} + x^{10}y^{10} + x^{10}y^{11} + x^{10}y^{12} + x^{11}y^{12}.$$

Proof:

From equation (22), The LM Polynomial of G arrives as follows:

$$LM(G;x,y) = \sum_{\beta \le \gamma} |E_{(\beta,\gamma)}|x^\beta y^\gamma = |E_{(4,6)}|x^4y^6 + |E_{(4,7)}|x^4y^7 + |E_{(5,8)}|x^5y^8 + |E_{(5,9)}|x^5y^9 + |E_{(5,10)}|x^5y^{10} + |E_{(6,6)}|x^6y^6 + |E_{(6,7)}|x^6y^7 + |E_{(6,8)}|x^6y^8 + |E_{(6,9)}|x^6y^9 + |E_{(7,7)}|x^7y^7 + |E_{(7,8)}|x^7y^8 + |E_{(7,9)}|x^7y^9 + |E_{(7,10)}|x^7y^{10} + |E_{(7,11)}|x^7y^{11} + |E_{(7,12)}|x^7y^{12} + |E_{(8,8)}|x^8y^8 + |E_{(8,9)}|x^8y^9 + |E_{(8,10)}|x^8y^{10} + |E_{(9,9)}|x^9y^9 + |E_{(9,10)}|x^9y^{10} + |E_{(9,12)}|x^9y^{12} + |E_{(10,10)}|x^{10}y^{10} + |E_{(10,11)}|x^{10}y^{11} + |E_{(10,12)}|x^{10}y^{12} + |E_{(11,12)}|x^{11}y^{12}.$$

$$= 2x^4y^6 + x^4y^7 + 3x^5y^8 + x^5y^9 + x^5y^{10} + 2x^6y^6 + 4x^6y^7 + 2x^6y^8 + x^6y^9 + 2x^7y^7 + 6x^7y^8 + x^7y^9 + 2x^7y^{10} + x^7y^{11} + x^7y^{12} + x^8y^8 + 3x^8y^9 + x^8y^{10} + 4x^9y^9 + x^9y^{10} + x^9y^{12} + x^{10}y^{10} + x^{10}y^{11} + x^{10}y^{12} + x^{11}y^{12}.$$

In the following theorem, the computation of Lakvir TIs of Remdesivir is attained using the LM polynomials, which is similar to the proof of Theorem 3.1.

Theorem 3.2.

Let G be a chemical graph of the Remdesivir drug. Then, we have:

(i) $Lv1(G)$= 706. (ii) $Lv2(G)$=5844. (iii) $Lv3(G)$= 2823.

(iv) $Lv4(G)$= 6.025. (v) $Lv5(G)$=349.7. (vi) $LvS(G)$= 11.02.

(vii) $Lv6(G)$=46258. (viii) $LvSD(G)$= 93.785. (ix) $LvISI(G)$= 146.83.

(x) $LvH(G)$= 7.55. (xi) $LvABC(G)$= 21.65. (xii) $HLv1(G)$= 11490.

(xiii) $HLv2(G)$=204785.

Lemma 3.3.

If G is a molecular graph of the Theaflavin drug, then:

$$LM(G;x,y) = 2x^5y^7 + 6x^5y^8 + 2x^5y^9 + 4x^7y^8 + 6x^8y^8 + 8x^8y^9 + 10x^8y^{10} + 3x^9y^{10} + 2x^9y^{11} + 2x^{10}y^{10} + x^{10}y^{11}.$$

Proof:

From equation (22), The LM Polynomial of G is arrived at as follows:

$$LM(G;x,y) = \sum_{\beta \le \gamma} |E_{(\beta,\gamma)}| x^{\beta} y^{\gamma} = |E_{(5,7)}|x^5y^7 + |E_{(5,8)}|x^5y^8 + |E_{(5,9)}| x^5y^9 + |E_{(7,8)}| x^7y^8 + |E_{(8,8)}|x^8y^8 + |E_{(8,9)}|x^8y^9 + |E_{(8,10)}|x^8y^{10} + |E_{(9,10)}|x^9y^{10} + |E_{(9,11)}|x^9y^{11} + |E_{(10,10)}|x^{10}y^{10} + |E_{(10,11)}|x^{10}y^{11}.$$
$$= 2x^5y^7 + 6x^5y^8 + 2x^5y^9 + 4x^7y^8 + 6x^8y^8 + 8x^8y^9 + 10x^8y^{10} + 3x^9y^{10} + 2x^9y^{11} + 2x^{10}y^{10} + x^{10}y^{11}.$$

In the following theorem, the computation of Lakvir TIs of Theaflavin has been obtained using the LM polynomials, which is similar to the proof of Theorem 3.1.

Theorem 3.3.

Let G be a chemical graph of Theaflavin drug. Then, we have:
(i) $Lv1(G)$= 760. (ii) $Lv2(G)$= 6482. (iii) $Lv3(G)$= 3162.
(iv) $Lv4(G)$= 5.745. (v) $Lv5(G)$= 377.23. (vi) $LvS(G)$= 11.4.
(vii) $Lv6(G)$= 54316. (viii) $LvSD(G)$= 95.07. (ix) $LvISI(G)$= 187.32.
(x) $LvH(G)$= 5.685. (xi) $LvABC(G)$= 21.54. (xii) $HLv1(G)$= 12806.
(xiii) $HLv2(G)$= 234694.

Lemma 3.4.

If G is a molecular graph of the Favipiravir drug, then:
$LM(G; x, y) = 3x^5y^7 + x^5y^8 + 2x^7y^7 + 2x^7y^8 + x^7y^{10} + 2x^8y^{10}.$
Proof:
From equation (22), the LM – Polynomial of G is arrived at as follows:

$$LM(G;x,y) = \sum_{\beta \le \gamma} |E_{(\beta,\gamma)}| x^{\beta} y^{\gamma} = |E_{(5,7)}|x^5y^7 + |E_{(5,8)}|x^5y^8 + |E_{(7,7)}| x^7y^7 + |E_{(7,8)}| x^7y^8 + |E_{(7,10)}|x^7y^{10} + |E_{(8,10)}|x^8y^{10}.$$
$$= 3x^5y^7 + x^5y^8 + 2x^7y^7 + 2x^7y^8 + x^7y^{10} + 2x^8y^{10}.$$

In the following theorem, the computation of Lakvir TIs of Favipiravir is achieved using the LM polynomials, which is similar to the proof of Theorem 3.1.

Theorem 3.4.

Let G be a chemical graph of the Favipiravir drug. Then, we have:
(i) $Lv1(G)$= 160. (ii) $Lv2(G)$= 1210. (iii) $Lv3(G)$= 585.
(iv) $Lv4(G)$= 1.57. (v) $Lv5(G)$= 79.3. (vi) $LvS(G)$= 2.91.
(vii) $Lv6(G)$= 8902. (viii) $LvSD(G)$= 22.84. (ix) $LvISI(G)$= 39.31.
(x) $LvH(G)$=1.55. (xi) $LvABC(G)$= 5.45. (xii) $HLv1(G)$=2380.
(xiii) $HLv2(G)$= 34039.

Lemma 3.5.

If G is a molecular graph of the Darunavir drug, then:
$LM(G; x, y) = 2x^5y^6 + 2x^5y^7 + x^5y^8 + 2x^6y^6 + 4x^6y^7 + x^6y^8 + 2x^6y^{10} + 5x^7y^7 + 4x^7y^8 + 3x^7y^9 + 3x^7y^{10} + 2x^8y^8 + 4x^8y^9 + 2x^8y^{10} + 2x^9y^{10} + 2x^{10}y^{10}.$
Proof:
From equation (22), The LM Polynomial of G is as follows:

$$LM(G;x,y) = \sum_{\beta \le \gamma} |E_{(\beta,\gamma)}| x^{\beta} y^{\gamma} = |E_{(5,6)}|x^5y^6 + |E_{(5,7)}|x^5y^7 + |E_{(5,8)}| x^5y^8 + |E_{(6,6)}| x^6y^6 + |E_{(6,7)}|x^6y^7 + |E_{(6,8)}|x^6y^8 + |E_{(6,10)}|x^6y^{10} + |E_{(7,7)}|x^7y^7 + |E_{(7,8)}|x^7y^8 + |E_{(7,9)}|x^7y^9 + |E_{(7,10)}|x^7y^{10} + |E_{(8,8)}|x^8y^8 + |E_{(8,9)}|x^8y^9 + |E_{(8,10)}|x^8y^{10} + |E_{(9,10)}| x^9y^{10} + |E_{(10,10)}|x^{10}y^{10}.$$
$$= 2x^5y^6 + 2x^5y^7 + x^5y^8 + 2x^6y^6 + 4x^6y^7 + x^6y^8 + 2x^6y^{10} + 5x^7y^7 + 4x^7y^8 + 3x^7y^9 + 3x^7y^{10} + 2x^8y^8 + 4x^8y^9 + 2x^8y^{10} + 2x^9y^{10} + 2x^{10}y^{10}.$$

In the following theorem, the computation of Lakvir TIs of Darunavir is explored using the LM polynomials, which is similar to the proof of Theorem 3.1.

Theorem 3.5.

Let G be a chemical graph of the Darunavir drug. Then, we have:
(i) $Lv1(G)$= 624. (ii) $Lv2(G)$= 4920 (iii) $Lv3(G)$=2292.
(iv) $Lv4(G)$=5.55. (v) $Lv5(G)$= 310.08. (vi) $LvS(G)$=10.61.
(vii) $Lv6(G)$=38288. (viii) $LvSD(G)$=84.05. (ix) $LvISI(G)$=154.1.
(x) $LvH(G)$= 5.52. (xi) $LvABC(G)$=19.81 (xii) $HLv1(G)$=9724.
(xiii) $HLv2(G)$=154086.

Lemma 3.6.

If G is a molecular graph of the Paxlovid drug, then:

$$LM(G;x,y) = x^5y^7 + 2x^6y^9 + 2x^6y^{10} + 2x^7y^8 + 7x^7y^9 + 2x^7y^{11} + x^8y^9 + x^8y^{10} + 3x^9y^9 + 4x^9y^{10} + x^9y^{11} + 4x^9y^{12} + x^{10}y^{11} + x^{10}y^{12} + 2x^{11}y^{12} + x^{11}y^{13} + 2x^{12}y^{13}.$$

Proof:
From equation (22), The LM Polynomial of G is as follows:

$$LM(G;x,y) = \sum_{\beta \le \gamma} |E_{(\beta,\gamma)}| x^{\beta} y^{\gamma} = |E_{(5,7)}|x^5y^7 + |E_{(6,9)}|x^6y^9 + |E_{(6,10)}| x^6y^{10} + |E_{(7,8)}| x^7y^8 + |E_{(7,9)}|x^7y^9 + |E_{(7,11)}|x^7y^{11} + |E_{(8,9)}|x^8y^9 + |E_{(8,10)}|x^8y^{10} + |E_{(9,9)}|x^9y^9 + |E_{(9,10)}|x^9y^{10} + |E_{(9,11)}|x^9y^{11} + |E_{(9,12)}|x^9y^{12} + |E_{(10,11)}|x^{10}y^{11} + |E_{(10,12)}|x^{10}y^{12} + |E_{(11,12)}| x^{11}y^{12} + |E_{(11,13)}|x^{11}y^{13} + |E_{(12,13)}| x^{12}y^{13}.$$
$$= x^5y^7 + 2x^6y^9 + 2x^6y^{10} + 2x^7y^8 + 7x^7y^9 + 2x^7y^{11} + x^8y^9 + x^8y^{10} + 3x^9y^9 + 4x^9y^{10} + x^9y^{11} + 4x^9y^{12} + x^{10}y^{11} + x^{10}y^{12} + 2x^{11}y^{12} + x^{11}y^{13} + 2x^{12}y^{13}.$$

In the following theorem, the computation of Lakvir TIs of Paxlovid has been done using the LM polynomials, which is similar to the proof of Theorem 3.1.

Theorem 3.6.

Let G be a chemical graph of the Paxlovid drug. Then, we have:
(i) $Lv1(G)$= 684. (ii) $Lv2(G)$=6588. (iii) $Lv3(G)$=3205.
(iv) $Lv4(G)$=4.13. (v) $Lv5(G)$=339.46. (vi) $LvS(G)$=8.88.
(vii) $Lv6(G)$=62652. (viii) $LvSD(G)$=76.43. (ix) $LvISI(G)$=168.53.
(x) $LvH(G)$=4.12. (xi) $LvABC(G)$=16.43. (xii) $HLv1(G)$=12998.

(xiii) $HLv2(G)$=307763.

Lemma 3.7.

If G is a molecular graph of the Molnupiravir drug, then:

$$LM(G;\, x, y) = x^4y^6 + 2x^5y^7 + 2x^5y^8 + 2x^5y^9 + x^6y^8 + 2x^7y^7 + 3x^7y^8 + x^7y^9 + x^7y^{10} + 2x^8y^8 + x^8y^9 + 2x^8y^{10} + 2x^9y^9 + x^9y^{10} + x^{10}y^{10}.$$

Proof:

From equation (22), The LM Polynomial of G is as follows:

$$LM(G;x,y) = \sum_{\beta \le \gamma} |E_{(\beta,\gamma)}|\, x^\beta y^\gamma = |E_{(4,6)}|x^4y^6 + |E_{(5,7)}|x^5y^7 + |E_{(5,8)}|\, x^5y^8 + |E_{(5,9)}|\, x^5y^9 + |E_{(6,8)}|x^6y^8 + |E_{(7,7)}|x^7y^7 + |E_{(7,8)}|x^7y^8 + |E_{(7,9)}|x^7y^9 + |E_{(7,10)}|x^7y^{10} + |E_{(8,8)}|x^8y^8 + |E_{(8,9)}|x^8y^9 + |E_{(8,10)}|x^8y^{10} + |E_{(9,9)}|x^9y^9 + |E_{(9,10)}|x^9y^{10} + |E_{(10,10)}|\, x^{10}y^{10}.$$

$$= x^4y^6 + 2x^5y^7 + 2x^5y^8 + 2x^5y^9 + x^6y^8 + 2x^7y^7 + 3x^7y^8 + x^7y^9 + x^7y^{10} + 2x^8y^8 + x^8y^9 + 2x^8y^{10} + 2x^9y^9 + x^9y^{10} + 1x^{10}y^{10}.$$

In the following theorem, the computation of Lakvir TIs of Molnupiravir is acquired using the LM polynomials, which is similar to the proof of Theorem 3.1.

Theorem 3.7.

Let G be a chemical graph of the Molnupiravir drug. Then, we have:

(i) $Lv1(G)$= 368. (ii) $Lv2(G)$=2825. (iii) $Lv3(G)$=1423.
(iv) $Lv4(G)$=3.26. (v) $Lv5(G)$=182.36. (vi) $LvS(G)$=6.19.
(vii) $Lv6(G)$=22920 (viii) $LvSD(G)$=50. (ix) $LvISI(G)$=90.36.
(x) $LvH(G)$=3.15. (xi) $LvABC(G)$= 11.66. (xii) $HLv1(G)$=5784.
(xiii) $HLv2(G)$=93057.

A more in-depth investigation of the LM Polynomial's properties may be expected to reveal novel, comprehensive insights about studying TIs. For visualizing the LM Polynomials, their 3D surface mapping is generated by GNU-OCTAVE 5.2.0. Figure 4 and Figure 5 represent the expressions of LM Polynomials for the drugs employed in COVID-19 and Omicron. Different colors are attributed to various surfaces. The surface is developed on a horizontal grid which is formed by taking the parameters x and y into account. The plots demonstrate how the polynomials behave differently depending on the parameters. By manipulating the LM polynomials with those parameters, TIs and their associated properties/functions can be controlled.

4. Applications

With major developments in the pharmacological sectors of several countries, many new drugs emerge every year and are authorized through early laboratory trials. A huge number of experiments are performed at the outset to evaluate those novel drugs for physicochemical behavior, toxicity, biological activity, and the severity of adverse effects they have on humans. This causes a massive workload in the lab, particularly in nations and territories (e.g., Africa and Southeast Asia) with limited resources and poor laboratory/experimental amenities.

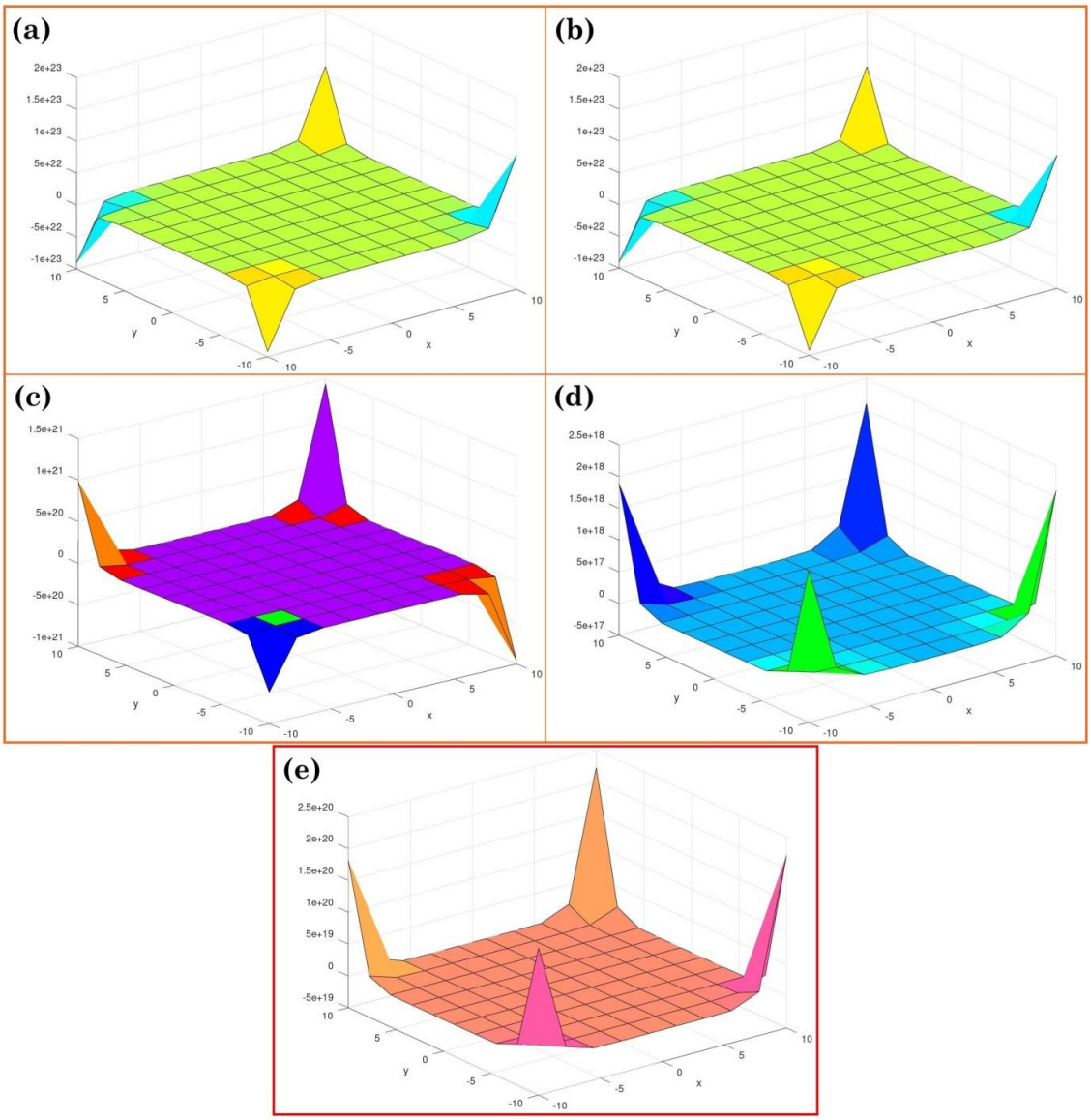

Figure 4. 3D surface plotting of **(a)** Arbidol; **(b)** Remdesivir; **(c)** Theaflavin; **(d)** Favipiravir; **(e)** Darunavir.

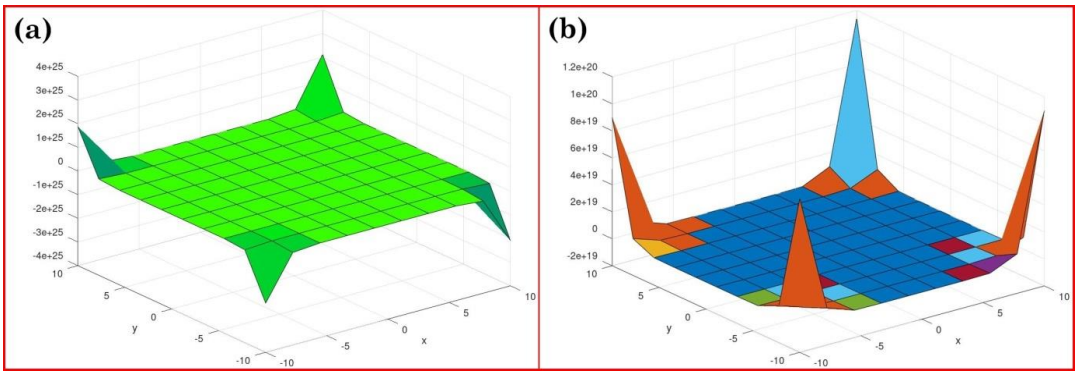

Figure 5. 3D surface plotting of **(a)** Paxlovid; **(b)** Molnupiravir.

Researchers correlated a tremendous sum of experimental observations with the structure of drugs/compounds in early chemical investigations and determined that the atomic/molecular arrangement of a compound has inherent relations with the properties it reveals [86-89]. In this regard, the analysis of TIs on the molecular mapping of compounds and their associated properties has been welcomed by most researchers and has been progressively applied to nanoscience, materials science, biology, medicine, and industrial chemistry [90-99].

5. Conclusion

We have initiated the open neighborhood degree sum along with the clique number. The novel topological indices mentioned in the work have strong correlations with molar volume, molar refraction, boiling point, acentric factor, entropy, critical pressure, mean radius, standard enthalpy of vaporization, enthalpy of vaporization, and heats of formation of octane isomers. The newly proposed Lakvir indices surpass some well-known indices and have better-discriminating power than octane isomers (exactly 1). We successfully established some novel M-Polynomials and obtained their accurate expressions for certain drugs employed in treating COVID-19 and Omicron. The computed results could lead to breakthroughs in the realm of structural chemistry as well as possible applications in predicting the properties of novel drugs during the initial phases of development. These polynomials can be applied to polymer compounds or complex network structures for future studies.

Funding

This research received no external funding.

Acknowledgments

This research has no acknowledgment.

Conflicts of Interest

There are no conflicts of interest.

References

1. Holmes, E.C.; Goldstein, S.A.; Rasmussen, A.L.; Robertson, D.L.; Crits-Christoph, A.; Wertheim, J.O.; Anthony, S.J.; Barclay, W.S.; Boni, M.F.; Doherty, P.C.; Farrar, J.; Geoghegan, J.L.; Jiang, X.; Leibowitz, J.L.; Neil, S.J.D.; Skern, T.; Weiss, S.R.; Worobey, M.; Andersen, K.G.; Garry, R.F.; Rambaut, A. The origins of SARS-CoV-2: A critical review. *Cell* **2021**, *184*, 4848–4856, https://doi.org/10.1016/j.cell.2021.08.017.
2. Shereen, M.A.; Khan, S.; Kazmi, A.; Bashir, N.; Siddique, R. COVID-19 infection: Emergence, transmission, and characteristics of human coronaviruses. *J. Adv. Res.* **2020**, *24*, 91–98, https://doi.org/10.1016/j.jare.2020.03.005.
3. Tyagi, P.K.; Tyagi, S.; Kumar, A.; Ahuja, A.; Gola, D. Contribution of Nanotechnology in the Fight Against COVID-19. *Biointerface Res. Appl. Chem.* **2021**, *11*, 8233–8241, https://doi.org/10.33263/BRIAC111.82338241.
4. Harapan, H.; Itoh, N.; Yufika, A.; Winardi, W.; Keam, S.; Te, H.; Megawati, D.; Hayati, Z.; Wagner, A.L.; Mudatsir, M. Coronavirus disease 2019 (COVID-19): A literature review. *J. Infect. Public Health* **2020**, *13*, 667–673, https://doi.org/10.1016/j.jiph.2020.03.019.
5. Mollaamin, F.; Esmkhani, R.; Monajjemi, M. Mutations in Novel COVID-19 Make it More Dangerous: Prevention Via Scientific Approaches. *Biointerface Res. Appl. Chem.* **2021**, *11*, 10546–10558, https://doi.org/10.33263/BRIAC113.1054610558.
6. Atiroğlu, V.; Atiroğlu, A.; Özsoy, M.; Özacar, M. Coronavirus Disease (COVID-19), Chemical Structure, Therapeutics, Drugs and Vaccines. *Biointerface Res. Appl. Chem.* **2022**, *12*, 547–566, https://doi.org/10.33263/BRIAC121.547566.
7. Atiroğlu, A.; Atiroğlu, A.; Özsoy, M.; Atiroğlu, V.; Özacar, M. COVID-19 in Adults and Children, Symptoms and Treatment. *Biointerface Res. Appl. Chem.* **2022**, *12*, 1735–1748, https://doi.org/10.33263/BRIAC122.17351748.

8. Çınar, F.; Ekinci, G. Investigation of the Effect of Comorbidity on Mortality in Patients with COVID-19: A Systematic Review and Meta-Analysis. *Biointerface Res. Appl. Chem.* **2022**, *12*, 5579–5590, https://doi.org/10.33263/BRIAC124.55795590.
9. V'kovski, P.; Kratzel, A.; Steiner, S.; Stalder, H.; Thiel, V. Coronavirus biology and replication: implications for SARS-CoV-2. *Nat. Rev. Microbiol.* **2021**, *19*, 155–170, https://doi.org/10.1038/s41579-020-00468-6.
10. Ramos-Casals, M.; Brito-Zerón, P.; Mariette, X. Systemic and organ-specific immune-related manifestations of COVID-19. *Nat. Rev. Rheumatol.* **2021**, *17*, 315–332, https://doi.org/10.1038/s41584-021-00608-z.
11. Belmehdi, O.; Hakkour, M.; El Omari, N.; Balahbib, A.; Guaouguaou, F.-E.; Benali, T.; El Baaboua, A.; Lahmoud, M.; Elmenyiy, N.; Bouyahya, A. Molecular structure, pathophysiology, and diagnosis of COVID-19. *Biointerface Res. Appl. Chem.* **2021**, *11*, 10215–10237, https://doi.org/10.33263/BRIAC113.1021510237.
12. Mao, R.; Qiu, Y.; He, J.-S.; Tan, J.-Y.; Li, X.-H.; Liang, J.; Shen, J.; Zhu, L.-R.; Chen, Y.; Iacucci, M.; Ng, S.C.; Ghosh, S.; Chen, M.-H. Manifestations and prognosis of gastrointestinal and liver involvement in patients with COVID-19: a systematic review and meta-analysis. *Lancet Gastroenterol. Hepatol.* **2020**, *5*, 667–678, https://doi.org/10.1016/S2468-1253(20)30126-6.
13. Benny, R.; Khadilkar, S.V. COVID 19: Neuromuscular Manifestations. *Ann. Indian Acad. Neurol.* **2020**, *23*, S40–S42, https://doi.org/10.4103/aian.AIAN_309_20.
14. Martinez, M.A. Efficacy of repurposed antiviral drugs: Lessons from COVID-19. *Drug Discov. Today* **2022**, *27*, 1954–1960, https://doi.org/10.1016/j.drudis.2022.02.012.
15. Hossain, M.J.; Jannat, T.; Brishty, S.R.; Roy, U.; Mitra, S.; Rafi, M.O.; Islam, M.R.; Nesa, M.L.; Islam, M.A.; Emran, T.B. Clinical Efficacy and Safety of Antiviral Drugs in the Extended Use against COVID-19: What We Know So Far. *Biologics* **2021**, *1*, 252–284, https://doi.org/10.3390/biologics1020016.
16. Yang, C.; Ke, C.; Yue, D.; Li, W.; Hu, Z.; Liu, W.; Hu, S.; Wang, S.; Liu, J. Effectiveness of Arbidol for COVID-19 Prevention in Health Professionals. *Front. Public Health* **2020**, *8*, 00249, https://doi.org/10.3389/fpubh.2020.00249.
17. Zhu, Z.; Lu, Z.; Xu, T.; Chen, C.; Yang, G.; Zha, T.; Lu, J.; Xue, Y. Arbidol monotherapy is superior to lopinavir/ritonavir in treating COVID-19. *J. Infect.* **2020**, *81*, e21–e23, https://doi.org/10.1016/j.jinf.2020.03.060.
18. Frediansyah, A.; Nainu, F.; Dhama, K.; Mudatsir, M.; Harapan, H. Remdesivir and its antiviral activity against COVID-19: A systematic review. *Clin. Epidemiol. Glob. Health* **2021**, *9*, 123–127, https://doi.org/10.1016/j.cegh.2020.07.011.
19. Grein, J.; Ohmagari, N.; Shin, D.; Diaz, G.; Asperges, E.; Castagna, A.; Feldt, T.; Green, G.; Green Margaret, L.; Lescure, F.-X.; Nicastri, E.; Oda, R.; Yo, K.; Quiros-Roldan, E.; Studemeister, A.; Redinski, J.; Ahmed, S.; Bernett, J.; Chelliah, D.; Chen, D.; Chihara, S.; Cohen Stuart, H.; Cunningham, J.; D'Arminio Monforte, A.; Ismail, S.; Kato, H.; Lapadula, G.; L'Her, E.; Maeno, T.; Majumder, S.; Massari, M.; Mora-Rillo, M.; Mutoh, Y.; Nguyen, D.; Verweij, E.; Zoufaly, A.; Osinusi Anu, O.; DeZure, A.; Zhao, Y.; Zhong, L.; Chokkalingam, A.; Elboudwarej, E.; Telep, L.; Timbs, L.; Henne, I.; Sellers, S.; Cao, H.; Tan Susanna, K.; Winterbourne, L.; Desai, P.; Mera, R.; Gaggar, A.; Myers Robert, P.; Brainard Diana, M.; Childs, R.; Flanigan, T. Compassionate Use of Remdesivir for Patients with Severe Covid-19. *N. Engl. J. Med.* **2020**, *382*, 2327–2336, https://doi.org/10.1056/NEJMoa2007016.
20. Aneja, R.; Odoms, K.; Denenberg, A.G.; Wong, H.R. Theaflavin, a black tea extract, is a novel anti-inflammatory compound. *Crit. Care Med.* **2004**, *32*, 2097–2103, https://doi.org/10.1097/01.ccm.0000142661.73633.15.
21. O'Neill, E.J.; Termini, D.; Albano, A.; Tsiani, E. Anti-Cancer Properties of Theaflavins. *Molecules* **2021**, *26*, 987, https://doi.org/10.3390/molecules26040987.
22. Laajala, M.; Reshamwala, D.; Marjomäki, V. Therapeutic targets for enterovirus infections. *Expert Opin. Ther. Targets* **2020**, *24*, 745–757, https://doi.org/10.1080/14728222.2020.1784141.
23. Hassanipour, S.; Arab-Zozani, M.; Amani, B.; Heidarzad, F.; Fathalipour, M.; Martinez-de-Hoyo, R. The efficacy and safety of Favipiravir in treatment of COVID-19: a systematic review and meta-analysis of clinical trials. *Sci. Rep.* **2021**, *11*, 11022, https://doi.org/10.1038/s41598-021-90551-6.
24. Chen, J.; Xia, L.; Liu, L.; Xu, Q.; Ling, Y.; Huang, D.; Huang, W.; Song, S.; Xu, S.; Shen, Y.; Lu, H. Antiviral Activity and Safety of Darunavir/Cobicistat for the Treatment of COVID-19. *Open Forum Infect. Dis.* **2020**, *7*, ofaa241, https://doi.org/10.1093/ofid/ofaa241.

25. Ghosh, A.K.; Dawson, Z.L.; Mitsuya, H. Darunavir, a conceptually new HIV-1 protease inhibitor for the treatment of drug-resistant HIV. *Bioorg. Med. Chem.* **2007**, *15*, 7576–7580, https://doi.org/10.1016/j.bmc.2007.09.010.
26. Gowrisankar, A.; Priyanka, T.M.C.; Banerjee, S. Omicron: a mysterious variant of concern. *Eur. Phys. J. Plus* **2022**, *137*, *100*, https://doi.org/10.1140/epjp/s13360-021-02321-y.
27. Mohapatra, R.K.; Sarangi, A.K.; Kandi, V.; Azam, M.; Tiwari, R; Dhama, K. Omicron (B.1.1.529 variant of SARS-CoV-2); an emerging threat: Current global scenario. *J. Med. Virol* **2022**, *94*, 1780–1783, https://doi.org/10.1002/jmv.27561.
28. Wen, W.; Chen, C.; Tang, J.; Wang, C.; Zhou, M.; Cheng, Y.; Zhou, X.; Wu, Q.; Zhang, X.; Feng, Z.; Wang, M.; Mao, Q. Efficacy and safety of three new oral antiviral treatment (molnupiravir, fluvoxamine and Paxlovid) for COVID-19 : a meta-analysis. *Ann. Med.* **2022**, *54*, 516–523, https://doi.org/10.1080/07853890.2022.2034936.
29. Saravolatz, L.D.; Depcinski, S.; Sharma, M. Molnupiravir and Nirmatrelvir-Ritonavir: Oral Coronavirus Disease 2019 Antiviral Drugs. *Clin. Infect. Dis.* **2023**, *76*, 165-171, https://doi.org/10.1093/cid/ciac180.
30. Malone, B.; Campbell, E.A. Molnupiravir: coding for catastrophe. *Nat. Struct. Mol. Biol.* **2021**, *28*, 706–708, https://doi.org/10.1038/s41594-021-00657-8.
31. Li, P.; Wang, Y.; Lavrijsen, M.; Lamers, M.M.; de Vries, A.C.; Rottier, R.J.; Bruno, M.J.; Peppelenbosch, M.P.; Haagmans, B.L.; Pan, Q. SARS-CoV-2 Omicron variant is highly sensitive to molnupiravir, nirmatrelvir, and the combination. *Cell Res.* **2022**, *32*, 322–324, https://doi.org/10.1038/s41422-022-00618-w.
32. Vitiello, A.; La Porta, R.; Trama, U.; Ferrara, F.; Zovi, A.; Auti, A.M.; Di Domenico, M.; Boccellino, M. Pandemic COVID-19, an update of current status and new therapeutic strategies. *Naunyn-Schmiedeberg's Arch. Pharmacol.* **2022**, *395*, 1159–1165, https://doi.org/10.1007/s00210-022-02265-9.
33. Pradhan, D.; Biswasroy, P.; Goyal, A.; Ghosh, G.; Rath, G. Recent Advancement in Nanotechnology-Based Drug Delivery System Against Viral Infections. *AAPS PharmSciTech* **2021**, *22*, 47, https://doi.org/10.1208/s12249-020-01908-5.
34. Ojha, P.K.; Kar, S.; Krishna, J.G.; Roy, K.; Leszczynski, J. Therapeutics for COVID-19: from computation to practices—where we are, where we are heading to. *Mol. Divers.* **2021**, *25*, 625–659, https://doi.org/10.1007/s11030-020-10134-x.
35. Agrawal, M.; Saraf, S.; Saraf, S.; Murty, U.S.; Kurundkar, S.B.; Roy, D.; Joshi, P.; Sable, D.; Choudhary, Y.K.; Kesharwani, P.; Alexander, A. In-line treatments and clinical initiatives to fight against COVID-19 outbreak. *Respir. Med.* **2022**, *191*, 106192, https://doi.org/10.1016/j.rmed.2020.106192.
36. Khan, Z.; Karataş, Y.; Rahman, H. Anti COVID-19 Drugs: Need for More Clinical Evidence and Global Action. *Adv. Ther*. **2020**, *37*, 2575–2579, https://doi.org/10.1007/s12325-020-01351-9.
37. de Almeida, S.M.V.; Santos Soares, J.C.; dos Santos, K.L.; Alves, J.E.F.; Ribeiro, A.G.; Jacob, Í.T.T.; da Silva Ferreira, C.J.; dos Santos, J.C.; de Oliveira, J.F.; de Carvalho Junior, L.B.; de Lima, M.d.C.A. COVID-19 therapy: What weapons do we bring into battle?. *Bioorg. Med. Chem.* **2020**, *28*, 115757, https://doi.org/10.1016/j.bmc.2020.115757.
38. Pavlopoulos, G.A.; Secrier, M.; Moschopoulos, C.N.; Soldatos, T.G.; Kossida, S.; Aerts, J.; Schneider, R.; Bagos, P.G. Using graph theory to analyze biological networks. *BioData Mining* **2011**, *4*, 10, https://doi.org/10.1186/1756-0381-4-10.
39. Gao, W.; Wang, Y.; Wang, W.; Shi, L. The first multiplication atom-bond connectivity index of molecular structures in drugs. *Saudi Pharm. J.* **2017**, *25*, 548–555, https://doi.org/10.1016/j.jsps.2017.04.021.
40. Gao, W.; Farahani, M.R.; Shi, L. THE FORGOTTEN TOPOLOGICAL INDEX OF SOME DRUG STRUCTURES. *Acta Med. Mediterr.* **2016**, *32*, 579–585.
41. Gao, W.; Wang, W.; Farahani, M.R. Topological Indices Study of Molecular Structure in Anticancer Drugs. *J. Chem.* **2016**, *1*, 3216327, https://doi.org/10.1155/2016/3216327.
42. Devillers, J.; Balaban, A.T. Topological Indices and Related Descriptors in QSAR and QSPR, 1st Edition, Devillers, J.; Balaban, A.T., Eds.; CRC Press, London, **1999**; https://doi.org/10.1201/9781482296945.
43. Hosamani, S.; Perigidad, D.; Jamagoud, S.; Maled, Y.; Gavade, S. Qspr Analysis Of Certain Degree Based Topological Indices. *J. Stat. Appl. Pro.* **2017**, *6*, 361-371, http://dx.doi.org/10.18576/jsap/060211.
44. Mondal, S.; Dey, A.; De, N.; Pal, A. QSPR analysis of some novel neighbourhood degree-based topological descriptors. *Complex Intell. Syst.* **2021**, *7*, 977–996, https://doi.org/10.1007/s40747-020-00262-0.
45. Kier, L.B.; Hall, L.H. Molecular Connectivity in Chemistry and Drug Research. Academic Press, New York, **1976**.

46. Wiener, H. Structural Determination of Paraffin Boiling Points. *J. Am. Chem. Soc.* **1947**, *69*, 17–20, https://doi.org/10.1021/ja01193a005.
47. Gutman, I. Degree-Based Topological Indices. *Croat. Chem. Acta.* **2013**, *86*, 351–361, http://dx.doi.org/10.5562/cca2294.
48. Gutman, I.; Trinajstić, N. Graph theory and molecular orbitals. Total φ-electron energy of alternant hydrocarbons. *Chem. Phys. Lett.* **1972**, *17*, 535–538, https://doi.org/10.1016/0009-2614(72)85099-1.
49. Shirdel, G.H.; Rezapour, H.; Sayadi, A.M. The Hyper-Zagreb Index of Graph Operations. *Iranian J. Math. Chem.* **2013**, *4*, 213–220, https://doi.org/10.22052/ijmc.2013.5294.
50. Furtula, B.; Gutman, I. A forgotten topological index. *J. Math. Chem.* **2015**, *53*, 1184–1190, https://doi.org/10.1007/s10910-015-0480-z.
51. Randic, M. Characterization of molecular branching. *J. Am. Chem. Soc.* **1975**, *97*, 6609–6615, https://doi.org/10.1021/ja00856a001.
52. Bollobás, B.; Erdös, P. Graphs of extremal weights. *Ars Combin.* **1998**, *50*, 225–233.
53. Fajtlowicz, S. On conjectures of graffiti-II. *Congr. Numer.* **1987**, *60*, 187–197.
54. Estrada, E.; Torres, L.A.; Rodríguez, L.; Gutman, I. AN ATOM-BOND CONNECTIVITY INDEX : MODELLING THE ENTHALPY OF FORMATION OF ALKANES. *Indian J. Chem. A Inorg. Phys. Theor. Anal.Chem.* **1998**, *37*, 849–855.
55. Sedlar, J.; Stevanović, D.; Vasilyev, A. On the inverse sum indeg index. *Discrete Appl. Math.* **2015**, *184*, 202–212, https://doi.org/10.1016/j.dam.2014.11.013.
56. Zhou, B.; Trinajstić, N. On a novel connectivity index. *J. Math. Chem.* **2009**, *46*, 1252–1270, https://doi.org/10.1007/s10910-008-9515-z.
57. Vukičević, D. Bond Additive Modeling 2. Mathematical Properties of Max-min Rodeg Index. *Croat. Chem. Acta* **2010**, *83*, 261–273.
58. Duraisami, M.S.; Parasuraman, K. Computational analysis of some degree based topological indices of cubic structured tungsten trioxide [l,m,n] nanomultilayer. *Nanosyst.: Phys. Chem. Math.* **2020**, *11*, 501–509, https://doi.org/10.17586/2220-8054-2020-11-5-501-509.
59. Duraisami, M.S.; Anburaj, D.B.; Parasuraman, K. Computing Vertex Degree-Based Multiplicative Version of Topological Indices for Tungsten Trioxide Nano Multilayer Structure in Nanotherapeutic Anti-Cancer Activity. *Biointerface Res. Appl. Chem.* **2022**, *12*, 2275–2284, https://doi.org/10.33263/BRIAC122.22752284.
60. Sankarraman, S.M. A Computational Approach on Acetaminophen Drug using Degree-Based Topological Indices and M-Polynomials. *Biointerface Res. Appl. Chem.* **2022**, *12*, 7249–7266, https://doi.org/10.33263/BRIAC126.72497266.
61. Sankarraman, S.M.; Ranjan, H. ON BOUNDS FOR CERTAIN CLOSED NEIGHBOURHOOD TOPOLOGICAL INDICES. *Adv. Appl. Math. Sci.* **2022**, *21*, 5597–5609.
62. Sankarraman, S.M.; Ranjan, H. Computing some Novel Closed Neighborhood Degree- Based Topological Indices of Graphene Structures. *Biointerface Res. Appl. Chem.* **2023**, *13*, 92, https://doi.org/10.33263/BRIAC131.092.
63. Sankarraman, S.M.; Ranjan, H. Quantitative Structure-Property Relationship Analysis on Priority PAHs Using Certain Closed Neighbourhood Topological Indices. *Biointerface Res. Appl. Chem.* **2023**, *13*, 306, https://doi.org/10.33263/BRIAC134.306.
64. Gutman, I. Geometric Approach To Degree-Based Topological Indices: Sombor Indices. *MATCH Commun. Math. Comput. Chem.* **2021**, *86*, 11–16.
65. Du, Z.; Jahanbai, A.; Sheikholeslami, S.M. Relationships between Randic index and other topological indices. *Commun. Comb. Optim.* **2021**, *6*, 137–154, https://doi.org/10.22049/CCO.2020.26751.1138.
66. Shao, Z.; Jahanbani, A.; Sheikholeslami, S.M. Multiplicative Topological Indices of Molecular Structure in Anticancer Drugs. *Polycycl. Aromat. Compd.* **2022**, *42*, 475–488, https://doi.org/10.1080/10406638.2020.1743329.
67. Monsalve, J.; Rada, J. Vertex-degree based topological indices of digraphs. *Discrete Appl. Math.* **2021**, *295*, 13–24, https://doi.org/10.1016/j.dam.2021.02.024.
68. Havare, Ö.Ç. Topological indices and QSPR modeling of some novel drugs used in the cancer treatment. *Int. J. Quantum Chem.* **2021**, *121*, e26813, https://doi.org/10.1002/qua.26813.
69. Pegu, A.; Deka, B.; Gogoi, I.J.; Bharali, A. Two generalized topological indices of some graph structures. *J. Math. Comput. Sci.* **2021**, *11*, 5549–5564.

70. Bondy, J.R; Murty, U.S.R. *Graph theory*. 1st Edition; Springer London, **2008**; 12–663, https://doi.org/10.1007/978-1-84628-970-5.
71. Trinajstić, N. Chemical Graph Theory. 2nd Edition; CRC Press, Boca Raton, **1992**; 1–352, https://doi.org/10.1201/9781315139111.
72. Shi, Y.; Dehmer, M.; Li, X.; Gutman, I.(Eds.) Graph Polynomials. 1st Edition; Chapman and Hall/CRC, New York, **2017**; 1-264.
73. Deutsch, E.; Klavzar, S. Computing Hosoya polynomials of graphs from primary subgraphs. *arXiv preprint arXiv:* **2012**, *1212.3179*, https://doi.org/10.48550/arXiv.1212.3179.
74. Ashrafi, A.R.; Manoochehrian, B.; Yousefi-Azari, H. On the PI polynomial of a graph. *Util. Math.* **2006**, *71*, 97–108.
75. Cancan, M.; Afzal, D.; Hussain, S.; Maqbool, A.; Afzal, F. Some new topological indices of silicate network via M-polynomial. *J. Discrete Math. Sci. Cryptogr.* **2020**, *23*, 1157–1171, https://doi.org/10.1080/09720529.2020.1809776.
76. Jahangeer Baig, M.N.; Jung, C.Y.; Ahmad, N.; Kang, S.M. On the M-polynomials and degree-based topological indices of an important class of graphs. *J. Discrete Math. Sci. Cryptogr.* **2019**, *22*, 1281–1288, https://doi.org/10.1080/09720529.2019.1691327.
77. Deutsch, E.; Klavžar, S. M-polynomial and Degree-based Topological Indices. *Iran. J. Math. Chem.* **2015**, *6*, 93–102, https://doi.org/10.22052/ijmc.2015.10106.
78. Kwun, Y.C.; Ali, A.; Nazeer, W.; Ahmad Chaudhary, M.; Kang, S.M. *M*-Polynomials and Degree-Based Topological Indices of Triangular, Hourglass, and Jagged-Rectangle Benzenoid Systems. *J. Chem.* **2018**, *2018*, 8213950, https://doi.org/10.1155/2018/8213950.
79. Khalaf, A.J.M.; Hussain, S.; Afzal, D.; Afzal, F.; Maqbool, A. M-Polynomial and topological indices of book graph. *J. Discrete Math. Sci. Cryptogr.* **2020**, *23*, 1217–1237, https://doi.org/10.1080/09720529.2020.1809115.
80. Raza, Z.; Essa K. Sukaiti, M. M-Polynomial and Degree Based Topological Indices of Some Nanostructures. *Symmetry* **2020**, *12*, 831, https://doi.org/10.3390/sym12050831.
81. Javaid, M.; Jung, C.Y. *M*-POLYNOMIALS AND TOPOLOGICAL INDICES OF SILICATE AND OXIDE NETWORKS. *Int. J. Pure Appl. Math.* **2017**, *115*, 129–152, http://dx.doi.org/10.12732/ijpam.v115i1.11.
82. Sarkar, P.; De, N.; Pal, A. On Some Neighbourhood Degree-Based Multiplicative Topological Indices and Their Applications. *Polycycl. Aromat. Compd.* **2022**, *42*, 7738-7753, https://doi.org/10.1080/10406638.2021.2007141.
83. García-Domenech, R.; Gálvez, J.; de Julián-Ortiz, J.V.; Pogliani, L. Some New Trends in Chemical Graph Theory. *Chem. Rev.* **2008**, *108*, 1127–1169, https://doi.org/10.1021/cr0780006.
84. Wagner, S.; Wang, H. Introduction to Chemical Graph Theory. CRC Press, Boca Roton **2008**.
85. Konstantinova, E.V. The Discrimination Ability of Some Topological and Information Distance Indices for Graphs of Unbranched Hexagonal Systems. *J. Chem. Inf. Comput. Sci.* **1996**, *36*, 54–57, https://doi.org/10.1021/ci9502461.
86. Dearden, J.C. The Use of Topological Indices in QSAR and QSPR Modeling. In Advances in QSAR Modeling: Applications in Pharmaceutical, Chemical, Food, Agricultural and Environmental Sciences, Roy, K., Ed.; Springer International Publishing, Cham, **2017**; 57–88, https://doi.org/10.1007/978-3-319-56850-8_2.
87. Mekenyan, O.; Bonchev, D.; Sabljic, A.; Trinajstic, N. Applications of Topological Indices to QSAR. The Use of the Balaban Index and the Electropy Index for Correlations with Toxicity of Ethers on Mice. *Acta Pharm. Jugosl.* **1987**, *37*, 75–86.
88. Hu, Q.N.; Liang, Y.Z.; Fang, K.-T. The matrix expression, topological index and atomic attribute of molecular topological structure. *J. Data Sci.* **2003**, *1*, 361–389.
89. Senbagamalar, J.; Baskar Babujee, J. Predicting Anti HIV Activity of Quinolone Carboxylic Acids Computation Approach Using Topological Indices. *Eur. J. Biomed. Inform.* **2013**, *9*, 9–13.
90. Basak, S.C.; Magnuson, V.R.; Niemi, G.J.; Regal, R.R.; Veith, G.D. Topological indices: their nature, mutual relatedness, and applications. *Math. Model.* **1987**, *8*, 300–305, https://doi.org/10.1016/0270-0255(87)90594-X.
91. Zeryouh, M.; Marraki, M.E.; Essalih, M. Some tools of QSAR/QSPR and drug development: Wiener and Terminal Wiener indices. In Proceedings of the 2015 International Conference on Cloud Technologies and Applications (CloudTech), 2-4 June 2015, **2015**; 1–4, https://doi.org/10.1109/CloudTech.2015.7336963.

92. Stankevich, M.I.; Stankevich, I.V.; Zefirov, N.S. Topological Indices in Organic Chemistry. *Russ. Chem. Rev.* **1988**, *57*, 191, https://doi.org/10.1070/RC1988v057n03ABEH003344.
93. Basak, S.C.; Mills, D.; Gute, B.D.; Grunwald, G.D.; Balaban, A.T. Chapter 6 - Applications of Topological Indices in the Property/Bioactivity/Toxicity Prediction of Chemicals. In Topology in Chemistry, Rouvray, D.H., King, R.B., Eds.; Woodhead Publishing, **2002**; 113–184, https://doi.org/10.1533/9780857099617.113.
94. Naeem, M.; Siddiqui, M.K.; Qaisar, S.; Imran, M.; Farahani, M.R. COMPUTING TOPOLOGICAL INDICES OF 2-DIMENSIONAL SILICON-CARBONS. *U.P.B. Sci. Bull., B* **2018**, *80*, 115–136.
95. Arockiaraj, M.; Clement, J.; Balasubramanian, K. Topological Indices and Their Applications to Circumcised Donut Benzenoid Systems, Kekulenes and Drugs. *Polycycl. Aromat. Compd* **2020**, *40*, 280–303, https://doi.org/10.1080/10406638.2017.1411958.
96. Munir, M.; Nazeer, W.; Nizami, A.R.; Rafique, S.; Kang, S.M. M-Polynomials and Topological Indices of Titania Nanotubes. *Symmetry* **2016**, *8*, 117, https://doi.org/10.3390/sym8110117.
97. Wang, Y.; Yousaf, S.; Bhatti, A.A.; Aslam, A. Analyzing the expressions for nanostructures via topological indices. *Arab. J. Chem.* **2022**, *15*, 103469, https://doi.org/10.1016/j.arabjc.2021.103469.
98. Ullah, A.; Qasim, M.; Zaman, S.; Khan, A. Computational and comparative aspects of two carbon nanosheets with respect to some novel topological indices. *Ain Shams Eng. J.* **2022**, *13*, 101672, https://doi.org/10.1016/j.asej.2021.101672.
99. Anil Kumar, K.N.; Basavarajappa, N.S.; Shanmukha, M.C.; Shilpa, K.C. Degree-Based Topological Indices on Asthma Drugs with QSPR Analysis during Covid-19. *Eur. J. Mol. Clin. Med.* **2020**, *7*, 53–66.